Photocatalytic degradation of methyl orange dye by $ZnO/TiO_2/CoFe_2O_4$ trapped in alginate beads

By

Miraso Marvelous Nzwanai

(R155257N)

Submitted in partial fulfilment of the requirements for the degree of

Bachelor of Science Honours in Chemical Technology to the

Department of Chemical Technology

Faculty of Science and Technology

Midlands State University

Supervisors:

Mr T. Nharingo and Dr U. Guyo

May 2019

DEDICATION

I dedicate this work to my parents for their unwavering support throughout the course of this degree.

ACKNOWLEDGEMENTS

This document would not be a success without the involvement of a great number of people. First and fore most I would like to sincerely acknowledge my esteemed supervisors Mr. T. Nharingo and Dr. U. Guyo for all the constructive criticism, unconditional support, guidance and assistance throughout the course of my study. To the MSU laboratory staff Mr. Mambanda, T. Kufakunesu, A. Mutomb and Bhavik, whose efforts can never be over emphasized. You sacrificed your precious time including late nights and weekends just to see this work perfect and complete. My heartfelt gratitude goes to the Midlands State University, Chemical Technology Department who helped me with meaningful and constructive ideas throughout the course of my degree. To my friend Miss M. Mutenheri, thank you for your patience, support and for strengthening me whenever I felt like giving up on my degree. Most importantly I would like to thank the RioZim (Cam and Motor Mine) officials for their special support and input, special mention going to Mrs O. Dhlamini and Mrs E. Dangeni without whom it would have been difficult for me to have access to the company's instrumentation. To my family especially Mr and Mrs Miraso, Evidence and Edson, your efforts, support and love are immeasurable, I am forever indebted to you God bless you. Last but not least my greatest thanks to a special person Mr T. Magora for the love, support and encouragement. All in all, I thank the Almighty God for all.

ABSTRACT

Azo dyes have become an immerging and difficult pollutant to the environment. Industrial activities have resulted in disposal of these toxic dyes in effluent and among them is methyl orange (MO) dye. Proper effluent treatment schemes have become a necessity so as to be able to reduce the potential toxicity issues regarding plant and animal life due to the rise in demand for clean and safe water. Several methods have been applied for the removal and degradation of MO dye but have proven to be inadequate. The purpose of this work was photocatalytic degradation of MO by a novel composite catalyst $ZnO/TiO_2/CoFeO_4$. ZnO was synthesized by sol-gel and $CoFe_2O_4$ via the co-precipitation method ZnO, $CoFe_2O_4$ and commercial TiO_2 was combined and trapped in alginate $ZnO/TiO_2/CoFe_2O_4$ was characterized for functional groups, thermal stability, size, morphology and surface crystallinity. Successful fabrication was shown by the presence of the O-H stretching, C-H stretching and the M-O stretching vibrations on the FTIR spectrum. The composite was thermally stable and the photocatalysts constituted 9% of the composite. Optimum conditions were pH 8, 240 min and 0.2 g catalyst dosage. The effective initial concentration was 10 mg/L. Complete decolorisation of 10 mg/L under optimum conditions giving up to 98.4% degradation. The mechanism of photocatalysis was indirect. The composite was stable as there was no change in the percentage composition in terms of the catalysts added which were 1.9% ZnO and 6.7% $CoFe_2O_4$ in both the recycled and the fresh composite. The composite can be reused up to 5 cycles giving significant degradation.

DECLARATION

I, **Miraso Marvelous Nzwanai R155257N**, hereby declare that I am the sole author of this dissertation. I authorize Midlands State University to lend this dissertation to other institutions or individuals for the purpose of scholarly research.

Signature……

Date ……

APPROVAL

This dissertation entitled "**Photocatalytic degradation of methyl orange dye by $ZnO/TiO_2/CoFe_2O_4$ trapped in alginate beads"** by Miraso Marvelous Nzwanai meets the regulations governing the award of degree of Chemical Technology of Midlands State University, and is approved for its contribution to knowledge and literal presentation**.**

Supervisor…….

Date…….

Table of Contents

LIST OF FIGURES

LIST OF TABLES

ABBREVIATIONS

AA Atomic Absorption Spectroscopy

AOPs Advanced Oxidation Processes

FTIR Fourier Transform Infrared Spectrometer

MO Methyl Orange

ROS Reactive Oxygen Species

SEM Scanning Electron Microscopy

SAED Selected Area Electron Diffraction

TGA Thermogravimetric analysis

UV Ultra Violet

UV-Vis Ultra violet visible spectroscopy

XRD X-ray Diffraction spectroscopy

ZTC $ZnO/TiO_2/CoFe_2O_4$ composite trapped in alginate beads

CHAPTER ONE

INTRODUCTION

1.1 Background

Waste water from industrial, agricultural and domestic use is highly contaminated with several pollutants which are organic, inorganic compounds and pathogenic microorganisms [1].These pollutants are harmful to both animals and plants, among them are organic dyes which have recently contributed great levels of contamination on the environment. The estimated amount of dyes that are lost in industries during the dyeing process is about 10-15% [2]. This has resulted in these dyes becoming one of the most form of environmental contamination since the presence of very minute concentrations of these dyes is clearly visible. Therefore, industrial operations involving the use of these dyes require proper effluent treatment schemes so as to be able to reduce the potential toxicity issues regarding plant and animal life. This has however become a significant contemporary challenge for many industries to define an economic process for treating their industrial effluents [3].Meanwhile the demand for clean portable water has greatly risen and this has resulted in increased attention towards the innovation of sustainable and easier ways of waste water purification and management [4].

One of the most commonly used dye in most industries is methyl orange (MO) which is an azo dye consisting of large amounts of aromatic compounds. MO is used as a dye in textile, pharmaceutical, food processing industries and as a colouring agent for the detection of hydrogen gas [5]. MO is highly toxic and soluble in water and it results in primary cancers involving

kidney, urinary bladder and liver due to its high mutagenic behavior [6]. The dye also affects the aesthetic merit, transparency, water-gas solubility, reduces light penetration through water and photosynthetic reactions are slowed down resulting in oxygen deficiency as well as deregulating the biological cycles of aquatic biota [7]. MO has the ability of altering the chemical and physical properties of the soil and this causes harm to flora and fauna since this deteriorates water bodies. They also cause death to soil organisms which results in the disturbance of agricultural production [8]. Therefore the removal of this dye in waste water becomes a cause for concern.MO dye is highly soluble [9], hence it is easily transported through sewers and rivers. The large amounts of aromatic compounds that are present in MO dye contribute to its stability. Due to high stability of the MO dye, the biological method of treatment becomes an ineffective method of degradation as the azo compounds are not aerobically degradable. However, under anaerobic conditions they undergo azo-linkage reduction which results in the production of aromatic amines which are colorless, toxic and carcinogenic [2].MO's solubility contributes to its high mobility hence removing it is difficult as small concentrations of the dye can contaminate a very large volume of water [8]. This results in the need for effective and safer methods of MO dye degradation.

Several methods have been employed for the treatment of waste waters containing organic dyes. These include adsorption [10], membrane filtration [11], chemical oxidation [12], photocatalytic degradation [5], [13]–[15], biological treatment methods [6], coagulation-flocculation [16] and a combination of different techniques [2]. These methods were proven to have several drawbacks hence their effectiveness on dye degradation and removal becomes limited [17], [18]. The use of adsorption and membrane filtration results in the concentration of the dye on one area or material whilst there is no permanent degradation of the dye compound. Employing chemical oxidation

and the azo linkage reduction under anaerobic conditions give rise to the release of more toxic products after the degradation process. The use of coagulation and flocculation results in the accumulation of huge amounts of sludge [19]. Most of the above mentioned methods have the disadvantage of high cost of treatment. The application of photocatalytic degradation in waste water management and treatment has been one of the most promising methods for detoxification of dyes and many other water pollutants [20]. Photocatalytic degradation has the ability of mineralizing the organic dyes completely into nontoxic compound and this process consumes less energy for the treatment procedure [21].

Photocatalysis using semiconductors has drawn significant attention towards the remediation of the environment resulting in complete/permanent degradation of the contaminants [22]. Advanced Oxidation Processes (AOPs) have received great attention in recent studies as alternative methods for water purification. In the course of the oxidation process, very reactive species are produced and these include hydroxyl radicals that oxidize several organic pollutants into less harmful products such as H_2O and CO_2 [2]. This is achieved by employing photocatalysts. These catalysts include transition metal oxides which have attracted considerable attention due to their interesting photochemical and photo-magnetic properties [23].

One of the most significant aspects of environmental photocatalysis is the selection of semiconductor materials such as ZnO. As one of the well- known photo catalyst, ZnO has received a great deal of attention in the degradation and complete mineralization of environmental pollutants [22]. Basically it is relatively cheap and provide high oxidizing power from photo- generated holes [24]. Important applications of ZnO nanopowders include electrophotography, photo printing, capacitors, protective coatings and anti-microbial activities. Apart from being a photocatalyst, ZnO acts as sterilizing agent as it exhibits anti-microbial

activity. The bacteria maturing in these waste waters is also destroyed by the ZnO nanoparticles [25].

TiO_2 has been greatly explored in the detoxification recalcitrant organic pollutants found in effluent water. It is the most widely studied catalyst due to its unique high photochemical reactivity, high photocatalytic activity, physical stability, chemical stability, low cost, availability, low environmental toxicity, electrical and optical properties [26]. TiO_2 is a strong oxidizing material because of its semiconducting property that is able to lower the activation energy for the degradation of organic pollutants. The band gap energy of TiO_2 is 3.2 eV which is large, this means more energy is required to excite an electron and thus the higher the band gap energy the lower the photocatalytic activity. When a photon of energy equal to or greater than this band gap is absorbed, an electron is promoted from the valence band to the conduction band creating a hole or an electron vacancy in the valence band [27]. However due to its large band gap, there is need to reduce the energy by coupling with other semiconductors so as to expand its effectiveness in photocatalysis [28]. Thus ZnO is used to come up with a composite material that allows the lateral movement of holes and electrons.

$CoFe_2O_4$ has also been extensively used in photocatalysis involving composite catalysts. These materials have been proven to show high adsorption capacities and surface area to volume ratio [29]–[31]. The superparamagnetic properties of these nanoparticles have also attracted great attention. It has been shown to exhibit high electromagnetic performance, excellent chemical stability and remarkable mechanical hardness behaviors. It therefore provides the composites with the magnetic property which supports the recovery of the catalyst for reuse [32].

According to Ucancus et al, [17] alginate is the salt of alginic acid and it is a natural polymer which is widely used as a component for entrapment. It is reported to be cheap, efficient, easy to prepare and has an open lattice structure for the fast diffusion of dye molecules during adsorption. Calcium alginate (CaAlg) has the ability to form stable hydrogels which can be used as a photocatalyst support. CaAlg can be modified so as to improve and enhance its chemical stability as well as adsorption capabilities [33]. Studies [34]–[36] have shown that alginate can be modified by the use of crosslinking agents which reduce the particle size, increase the surface area and adsorption. Crosslinking agents that can be applied include $MgCl_2$, $AgCl_2$, $ZnCl_2$ and $CaCl_2$ [37]. Recent works done has proven the feasibility of using CaAlg as the support material in the removal and degradation of dyes [34]–[36].

Alginate has also several important features such as non-toxicity, hydrophilicity, biocompatibility and anti-bacterial properties [38], [39]. In photocatalytic degradation of organic pollutants, the carbon-based nanostructures act both as electron-acceptor and as electron-transport materials. The materials also facilitate the migration of photo-generated electrons, slowing down the charge recombination, thus enhancing the lifetime of electron–hole pairs and improving the photocatalytic efficiency [40]. The ZnO, TiO_2 and $CoFe_2O_4$ nanoparticles have excellent photocatalytic activity that is more effective for the degradation of organic pollutants. The carbon spheres on the other hand possess impressive adsorption ability for dyes and heavy metals due to the pores generated during the carbonization process [41]. The incorporation of these materials together can complement one another with their advantages and produce an effective material for the degradation of MO dye treatment. Therefore, the alginate was used in the formation of beads in this current study. The resulting composite contained $ZnO/TiO_2/CoFe_2O_4$ (ZTC) nanocomposite trapped in alginate beads.

The combination of ZnO, TiO_2 and $CoFe_2O_4$ trapped in alginate derived spheres can possibly yield an effective composite for the photocatalytic degradation of MO dye to simpler and less harmful products hence the focus of this study. The major disadvantages of using individual catalysts which include the large band gap in ZnO is countered by combining it with TiO_2. This endorses the splitting of photo-induced electron holes by preventing electron hole recombination and thus photocatalysis is enhanced [2]. The other major issue with the implementation of heterogeneous photocatalysis is the difficulty in the recovery and reuse of the catalyst as they are difficult to separate from the purified water. This is corrected by the addition of the magnetic $CoFe_2O_4$. Therefore, the fabrication of the $ZnO/TiO_2/CoFe_2O_4$ nanocomposite can be applied in the photocatalytic degradation of MO dye. The fabricated composite was characterized and photocatalytic degradation studies carried out so as to monitor the rate and effectiveness of the degradation. The recovery, reuse and stability of the nano-composite were established in this study.

1.2 Aim

The aim of the study was to synthesize $ZnO/TiO_2/CoFeO_4$nano composite trapped in alginate beads and apply it in photocatalytic degradation of methyl orange dye.

1.3 Specific Objectives

1) To fabricate $ZnO/TiO_2/CoFe_2O_4$ nano-composite trapped in alginate beads.
2) To characterize the composite beads with respect to the functional groups, thermal stability, porosity, surface crystallinity and morphology.

3) To optimize pH, initial concentration, exposure time and catalyst dosage for the photocatalytic degradation of MO.
4) To investigate the mechanism of photocatalytic degradation of MO.
5) To perform recovery, reusability and stability studies of the nano-composite.

1.4 Problem Statement

The impact caused by water pollution to the livelihoods of animals and plans are considered as a major global problem which requires effective techniques to treat effluent water [42]. Statistics suggests that the leading cause of deaths and diseases worldwide is attributed to water pollution and this account s for the death of over 15000 people each day worldly from organic pollutants in water [26]. A major concern in water treatment is that the presence of very minute concentrations of dyes in water is highly visible. This affects the aesthetic merit, transparency, water-gas solubility, reduces light penetration through water and photosynthetic reactions are slowed down resulting in oxygen deficiency as well as deregulating the biological cycles of aquatic biota [22]. Organic dyes have the ability of altering the chemical and physical properties of soil and this causes harm to flora and fauna in the environment since this deteriorates water bodies. They also cause death to soil organisms which results in the disturbances of agricultural production. Due to the high poisonous state of these azo dyes to the ecosystem and mutagens they pose acute threat to chronic effects on organisms but the extent depends on the time of exposure and the concentration of the dye [43].

MO dye is a very important type of a dye which is employed in several important industrial activities. The total eradication of the use of MO dye cannot be possible hence there is need for invention of proper, cheaper and applicable methods of degradation of the dye [5]. MO dye is an

azo dye, which contains aromatic rings which make it very stable, hence biological methods of degradation, becomes ineffective. MO is highly soluble in water and that makes it very mobile in water resulting in contamination of a large portion of water upon exposure from a single point of contact. This compound is also resistant to aerobic degradation and under anaerobic degradation it forms aromatic amines which are colorless but toxic and carcinogenic [14], [44]. Due to the stability of the dye, it can stay in the water for a long period of time if not treated with effective measures. There is also enough evidence presenting the harmful effects of MO dyes on animals which include the primary cancers involving kidney, urinary bladder and liver due to its high mutagenic behavior [45]. MO used in the textile industry cause allergies such as contact dermatitis and respiratory diseases, allergic reactions in eyes skin, chemosis, lacrimation, exopthamlmose, permanent blindness, rhabdomyolysis, acute tubular necrosis supervene, vomiting gastritis, hypertension, oedema of the face, neck and pharynx [44]. MO contains aromatic amines which can be metabolized by sweat or water and they can easily be absorbed by the skin and other exposed areas such as the mouth. Assimilation through ingestion in the mouth is faster and the harm caused is potentially high since large amounts of the dye is consumed in a small time frame [14].

Several methods that have been employed are expensive and less effective. The use of individual catalysts for the degradation has resulted in several drawbacks which include large band gap, catalyst toxicity, difficulties in recovery of the catalysts and reusability. The band gap energies for commonly used semiconductors are; TiO_2 (3.32 eV), ZnO (3.4 eV), CuO (2.0 eV), WO_3 (2.5eV) [43] hence there is need to energize them before applying the catalysts for photocatalytic degradation. The use of adsorbents in dye removal results in further concentration of the dyes through adsorption and this causes more contamination on the environment. Some of the

degradation processes used produce more toxic products than the individual dye [9], [46]. Therefore, this results in conventional methods failing to meet the key objective of treating the water for safe use.

1.5 Justification

Photocatalysis is an effective method since it is more efficient and can easily be applied [14], [44].The process is less costly due to the application of nanoparticles made from metal oxides which uses energy from the sun, and it contributes less toxic waste to the environment. The proposed method is more advantageous over adsorption as it results in complete degradation of the dye forming harmless products of water and carbon dioxide [47].

Several researchers have recently coupled metal oxides for water purification and spitting applications. The results show that semiconductor composite photocatalysts in all photocatalytic degradation of organic pollutants were more active than individual catalysts [48], [49]. While most of these reports on composite catalysts acknowledge the role of band gap offsets, detailed investigations of reaction mechanisms are often not undertaken, nor has the nature of these energy offsets been thoroughly scrutinized. The combination of the catalysts results in the lateral movement of holes [50]. The movement and incorporation of holes in a good catalyst with a smaller band gap, populating the other catalyst improves the movement of electrons which results in the supply of electrons to the other catalyst with a larger band gap [3], [51]. This study focuses on the combination of individual photocatalysts and taking their advantages into consideration towards the photocatalytic degradation of MO dye. Also the properties of individual catalyst material plays important roles and thus, numerous catalysts have been combined to achieve the goal [43].Limitations of individual photocatalysts will be countered and

catered for through the combination [2]. The inclusion of a magnetic photocatalyst, $CoFe_2O_4$ in the composite will aid for the recovery and reuse of the composite [32]. Also the narrow band gap of TiO_2 and $CoFe_2O_4$ enables an efficient degradation method which is not power consuming as well the ability to perform under sunlight [52]. This method is hence less toxic, less costly and safe to apply as it makes use of photocatalysts such as ZnO and TiO_2, therefore this makes the composite applicable to water treatment [2] and hence justifies the use of $ZnO/TiO_2/CoFe_2O_4$nano composite trapped in alginate beads for the photocatalytic degradation of MO dye.

Currently, the demands for clean and safe water have hastily increased all over the world and in order to provide the required amount of water with ultimate quality, the commonly engaged purification methods are not adequate and thus effective methods are greatly needed. Treating effluent water using photocatalysis has proven to be the most advanced and effective method since a small amount of the catalyst material is required which results in the generation of small amounts of less harmful by-products. Due to the ability of metal oxides to eliminate the toxic contaminants , metal oxides are the most suitable materials for the photocatalytic reactions [2]. The use of heterogeneous photocatalysis is possibly the proper technique for the degradation of these organics as it permits the mineralization of organic molecules to CO_2 and H_2O and it prevents secondary pollution [5]. Also the method is environmental friendly, less expensive as it makes use of the sunlight, produces smaller and less toxic products [7].

MO is an important example of an azo dye which is widely used in several industrial activities. Therefore the total eradication of MO from industrial activities is impossible and hence there is a great need for effective and cheap methods of treating the excess dyes found in waste water [5].

This justifies the use of the $ZnO/TiO_2/CoFe_2O_4$ nano-composite trapped in alginate beads in the photocatalytic degradation of MO dye.

CHAPTER 2

LITERATURE REVIEW

2.0 Introduction

The synthesis of nanoparticles for photocatalysis has been tried by several researchers for centuries with some extent of success and failures. This chapter reviews an in depth analysis of the work that was done in the past. An insight to the scope of this study was derived from these previous studies in the photocatalytic degradation of organic dyes by the use of semiconductor catalysts. This was used to come up with relevant concepts on the application of nanoparticles as catalysts in the degradation of MO dye for this study.

2.1 Chemistry of organic dyes

The advancement of industrialization has seen enormous amounts of waste containing dyes being disposed into the environment. These dyes cause environmental pollution causing harm to animals and plants. These synthetic dyes contain azo linkages which give them the bright color due to the presence of one or more azo (-N=N-) groups associated with substituted aromatic structures [53].These are chemicals which upon binding to a material give color. They are ionic,

aromatic organic compounds which have structures that contain aryl rings with delocalized electrons. Color produced by dyes are as a result of the chromophore group which is a radical configuration consisting of conjugated double bonds with delocalized electrons [6]. The chromogen which is the aromatic structure usually consisting of benzene, anthracene or naphthalene rings is part of the chromogen chromophore structure along with an auxochrome [6]. A stronger alteration of the maximum absorption of the compound and provision of bonding affinity is as a result of the presence of ionizing groups known as auxochromes. Waste water colored with dyes increases due to the production of the dyes as well as their use in textile and other industries [54].

2.2 Chemistry of MO dye

MO is one of the well-known anionic dye and is usually used as an indicator in laboratories, textiles and other industrial activities. MO (Fig 2.0) is also known as 4-[4-(Dimethylamino) phenylazo] benzenesulfonic acid sodium salt, Acid Orange 52, Helianthin, Orange III. It is an anionic dye belonging to the azo group of dyes. MO in effluent discharges has to be removed because of its high toxicity be it the dye itself or the breakdown products of the dye. Furthermore, MO is difficult to remove due to its high stability hence has low biodegradability [55].

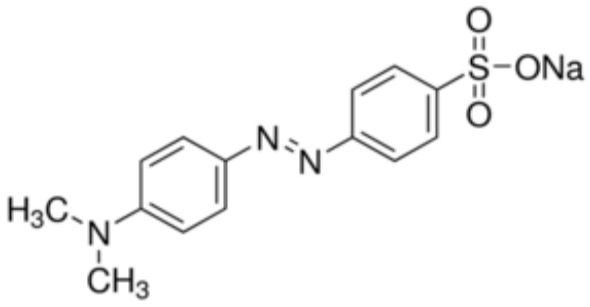

Figure 2.0 Structure of MO dye [50]

MO is very sensitive to pH and is orange at pH5-6, pH lower than 5 it is red in solution and at alkaline pH above 7 it exhibits a pale orange-yellow color. Due to its sensitivity to pH it is usually used as an indicator in acid base titrations. MO is used in textile dyeing and this results in more of it being released into the environment [56].

2.3 Effects of MO on the environment

Due to the aromatic rings associated with MO, it is a very stable compound such that biological treatment of waters containing MO is inefficient. Under anaerobic conditions it undergoes azo linkage reduction which results in the generation of toxic, colorless and carcinogenic aromatic amines [2]. MO is synthesized with high solubility in water, hence this results in its increased mobility. Since it is highly mobile, the exposure of a small concentration to a water source results in contamination of huge amounts of water. It is stable and therefore it can stay in the water for decades if effective treatment procedures are not done. This results in damage on plants and animals. MO causes development of primary cancers due to its mutagenic behaviour [45]. MO used in the textile industry cause allergies such as contact dermatitis and respiratory diseases, allergic reactions in eyes skin, chemosis, lacrimation, exopthamlmose, permanent blindness, rhabdomyolysis, acute tubular necrosis supervene, vomiting gastritis, hypertension, vertigo and upon ingestion, oedema of the face, neck and pharynx [22]. It contains aromatic amines which can be metabolized by sweat or water and they can easily be absorbed by the skin and other exposed areas such as the mouth. Assimilation through ingestion in the mouth is faster and the harm caused is potentially high since large amounts of MO is consumed in a short space of time [14].

Yagub [57] indicated that dyes causes a blockage in the light penetration through water sources. This causes an effect on the photosynthetic activities in aquatic life. Lack of photosynthesis gives rise to a decrease on the carbohydrate production in plants resulting in death of these plants. Dead aquatic plants consume most of the oxygen present in the water and hence, lack of photosynthesis results in less oxygen being available to aquatic animals. This disrupts the food chain of aquatic life and they end up dying [12]. These dyes also contain metals, aromatics and other toxic groups which cause harm to the aquatic life [58].

2.4 Conventional treatment methods of effluent water containing dyes

Several techniques have been used to remove dyes from coloured water. These methods include biological treatment, enzymatic, sonochemicals, nanotechnology, photocatalysis, coagulation and flocculation [12]. Some of these methods have shown limitations due to high operational costs and other process related problems. Most of these techniques are not able to completely destroy the contaminants but instead transfer the dyes from the solution to the adsorbent; as such, the dyes are transformed into their carcinogenic, mutagenic, or toxic intermediates, which cause secondary pollution. Thus, inexpensive and environment-friendly processes for the complete conversion of pollutants must be developed [59].

2.4.1 Biological water treatment methods

Biological waste water treatment is considered as a more natural treatment process compared to other waste water treatment methods such as chemical oxidation that requires addition of chemicals. Biological/ natural treatment makes use of the aerobic and anaerobic degradation. Microorganisms consume the complex organic materials found in waste water thereby turning them into simpler products. This process prepares the water for further treatment. It involves the

chemical dissolution of materials by bacteria or other biological means and is also known as biodegradation[20]. Biological treatment methods are cheap and easy to apply. This method does not require energy for the decomposition of the waste. Therefore, little or no capital is required to apply biological treatment methods [16]. MO is synthetic and very stable therefore it does not undergo biodegradation. However, under anaerobic conditions, MO undergoes azo linkage reduction which results in production of more toxic end products. Therefore, biological treatment of waste water containing MO dye and other azo dyes cannot be applied [60]. Conventional biological treatment of waste water has certain disadvantages which include sludge production, incomplete degradation of the pollutant dyes as well as production of more toxic products which cause secondary pollution [20].

2.4.2 Physico-chemical methods of treating dye contaminated effluent water

The traditional methods of water treatment that include adsorption onto activated carbon, reverse osmosis, ultrafiltration, ion exchange on synthetic resins, electrochemical and coagulation by chemical agents have been used for the removal of dyes. These techniques have been effective alternative methods of dye removal from contaminated waste water [57]. Adsorbents are prepared from affordable materials hence low capital investments, also the design is simple as well as the applicability of the method [48]. Consequently, the reusability of the materials used can be difficult since the dye adsorbed remains on the material. The handling or disposal of the adsorbent after use should be carefully monitored as this results in secondary pollution of the environment. This method has only been successful in the transference of the dye species from the water to a solid surface thereby reducing the effect caused by the dyes [27]. Thus the used adsorbents cannot be disposed into the environment. Special treatment of the adsorbent and the

solid waste generated is required and thus makes the techniques more costly [61]. Coagulation involves addition of a coagulant into the colloidal dispersion. Rapid breakage or rearrangement and aggregation of particles occurs. This method can be accomplished by compression of the electrical double layer, neutralization of the charge and adsorption, precipitation, adsorption and inter-particle bridging. Aluminum sulphate, ferric chloride and polyaluminum chloride are some of the commonly used coagulants in the industry. These chemical substances pose several impacts which include increased metal concentration in water, voluminous toxic sludge and detrimental effects on human health. Aluminum based coagulants have been reported to be associated with the development of Alzheimer's disease in humans. The disadvantages of these conventional methods, the use of more ecofriendly and cheaper methods of dye removal is required in order to substitute these techniques [16].

2.4.3 Advanced oxidation processes (AOPs) in the degradation of dyes

Vincenzo [12] mentioned that AOPs are used as a technique usually employed to improve the overall efficiency of the removal of organic dyes from effluent waters which has undergone pre-treatment via the biological method. AOPs can be used as pre- and/or post treatment of biological treatment systems. This technique is based on the chemistry of hydroxyl radicals (OH•). These are non-selective reactive species and they are able to mineralize organic pollutants into CO_2 and H_2O and inorganic ions. The mechanism behind the degradation of the pollutant involves the oxidation reaction between the radicals and the contaminant. Several processes are involved in the generation of the radicals which include sonolysis, ozone-based process, Fenton based reactions, heterogeneous photocatalysis. The method of free radical generation is specific for each process [62].

Cesaro etal [12]mentioned that sonochemical process involves the application of ultrasound (US). US is propagated into a liquid and formation of cavitational bubbles and their collapse is associated to both chemical and physical effects. Chemical ultrasonic effects are predominant at high frequencies due to the formation of free radicals. The reaction of the radicals and the organic substance then takes place when the radicals move to the liquid-gas interface. When higher concentrations are present, they recombine with each other forming H_2O_2, and is an oxidative agent hence degradation of contaminants occurs [12], [20]. Sonolysis is however disadvantageous since it requires high energy consumption. Contrarily, ozonation process has proven to be a strong oxidizing power involving short reaction times thus permitting the treatment of large volumes of effluent water. Ozone is an unstable element in aqueous media which decomposes spontaneously. Its decomposition is a complex mechanism which involves the production of hydroxyl free radicals. Subsequently the degradation of organic dye pollutants occurs both by ozone itself and radicals [63].

Ozone can be combined with UV radiation in the wavelength range of 200 and 280nm. The main disadvantage is the association of the small molar extinction coefficient of H_2O_2. Thus a relative small fraction of incident of light is used particularly when organic substrates will act as inner filters [16]. The Fenton based processes can involve the use of H_2O_2. The formation of radicals takes place under the reaction of H_2O_2 and iron in water under acidic conditions. Heterogeneous photocatalysis is a reaction that involves light and it is accelerated by the action of a catalyst. One of the most employed and highly effective catalyst is TiO_2. The mechanism results from light irradiation of the catalyst gives rise to the transition of electrons from the valence to the conduction band. Redox reactions with compounds absorbed on the photocatalyst takes place as

a result of the holes created in the valence band by the migration of electrons and the holes [12], [63].

2.5 Nanotechnology in waste water treatment

Nanotechnology has been an area of study for several researchers. Synthesized nanoparticles show unique physical properties such as large surface area to volume ratio or high interfacial reactivity, high magnetic, electrical and optical properties [64]. Nanotechnology has opened up a number of new avenues due to these special properties exhibited by nanoparticles. Advanced nanoparticle research has resulted in materials that exhibit specific interaction with contaminants in water, gases and soil. The application of these nano-sized materials gives effective approaches in overcoming the problems of environmental pollution. The application of these small sized nanoparticles provides a larger surface to volume ratio thus better surface reaction is provided. This has seen environmental protection towards pollution going to another level [4], [65]. However, the application of these individual particles have several limitations that involve difficulties in recovery and reuse of these particles thereby resulting in the loss of the materials. Heterogeneous use of these nanoparticles especially in photocatalysis is limited due to other problems such as larger band gaps in some nanoparticles as well as toxicity of some particles when they are not recovered from the effluent source. This makes the techniques more expensive since more capital is required to synthesize other nanoparticles. To alleviate this problem, researchers came up with the idea of fabrication of nanocomposites. This involves the synthesis of hybrid nanocomposites through impregnating, coating or mixing several particles with different properties so as to come up with a composite that has excellent properties towards the intended application [29].

2.6 Photocatalysis

Photocatalysis is the amalgamation of photochemistry and catalysis. During this process, light and catalysts are concurrently used to support or speed up a chemical reaction. Photocatalysis is divided into two classes which are the homogeneous and heterogeneous catalysis. Under homogeneous catalysis, metal complexes are mainly used as catalysts (transition metal complexes such as Fe, Cu, Co and others). Homogeneous catalysis involve the generation of hydroxyl radicals which will react with the organic pollutants [27]. A comparison with heterogeneous catalysis, it possesses several advantages over other competing processes. These include the complete mineralization of the pollutants, low cost and the ease of operation [27].

Semiconducting materials such as TiO_2, ZnO, SnO_2 and CeO_2 mainly exhibit heterogeneous photocatalyst behaviour. This is due to their favorable combination of an electronic structure that is characterized by a filled valence band and an empty conduction band. Hariharan [66] also alluded the other advantages include their ability to absorb light, excited states lifetime and charge transport characteristics. Studies have established that an excellent semiconductor photocatalyst should be photoactive, able to utilize visible and/or near UV light, biologically and chemically inert, photo stable, inexpensive and non-toxic. Photocatalysis using semiconductors has proven to be a promising alternative technique with various applications in environmental systems [24].

The major steps of semiconductor photocatalysis are as follows; the light energy in the form of photons hit the semiconductor catalyst surface and if the incident ray energy is equal or exceeds the band gap energy of the semiconductor, the valence band electrons are agitated and move towards the conduction band [27]. Holes are created in the valence band of the semiconductor which can oxidize donor molecules and react with water molecules to generate hydroxyl radicals.

These hydroxyl radicals possess strong oxidizing power which is responsible for pollutants degradation. Electrons on the conduction band then react with dissolved oxygen to generate superoxide ions. The redox reactions taking place are induced by these electrons. Thus the holes and electrons undergoes successive oxidation and reduction reactions with any species that can be adsorbed on the surface of the semiconductor to produce less harmful products [27], [52], [64].

Dyes have been reported as one of the major sources of contamination worldwide. To reduce their effects, studies have been focused on photocatalysis. This process uses light energy to convert organic dyes to harmless compounds [67]. Lately, photocatalysis has been conveniently applied for the treatment of contaminated waste water through the degradation of dye pollutants. This is due to the ability of the technique to mineralize organic dyes completely into H_2O, CO_2 and mineral acids avoiding secondary pollution. A photocatalyst is rendered efficient only if it is able to facilitate the competition of different interphase processes involving the e^- and h^+ reactions with species adsorbed, lessening the rate of electron-hole recombination [46]. This is achieved by transfer of electrons from the valence band to the conduction band of a semiconductor surface on illumination with an appropriate wavelength of light. These generated excited electrons react with oxygen or water to generate superoxide anions and hydroxide radicals. The generated species possess high oxidizing power to degrade several compounds including the azo dyes [68].

Metal semiconductor materials, such as TiO_2, ZnO, Fe_2O_3, CdS, CeO_2 and ZnS, are used as photocatalysts. These materials are cost-efficient, environmental friendly and efficient have been used to get rid of the environmental pollution problems. It has been reported that among these semiconductors, ZnO has been proven to exhibit greater efficiency in photocatalytic degradation

of some organic dyes than TiO_2. Therefore, ZnO has become another photocatalyst being widely applied in water treatment second to TiO_2as most researchers have been motivated to study ZnO and its applications in photo catalysis [69].

2.6.1 ZnO as a photocatalyst

Most metal oxides have a large range and so is their applications. Nanostructured ZnO has been found to display appealing nano-morphological, functional, biocompatible, non-toxic and catalytic properties. The demand for ZnO nanopowders is greatly increasing because of its wide use in industries [70]. ZnO has found a wider range of applications due to its properties which include UV filtration, anti-corrosion, antibacterial and catalytic properties. It has been recently applied in sunscreens as an UV resistant additive. Other important applications of ZnO nanopowders include electrophotography, photo printing, capacitors, protective coatings, anti-microbial, and conductive thin-films in LCDs, solar cells, and blue laser diodes [71].

ZnO represents the n-type semiconductor and it has a wide band gap of 3.37 eV. The N-type semiconductor behavior is due to the ionization of excess zinc atoms in interstitial positions as well as the oxygen vacancies [72]. The surface defects on metal oxides play an important role in photocatalysis as they increase the number of active sites [73]. As a result of these properties of ZnO, it has been greatly applied in photocatalysis [2], [74]. ZnO produces electron-hole pairs under UV light or visible light irradiation. The electron and hole produced can interact with the O_2 adsorbed on the surface of the photocatalyst and water to generate radicals O_2• and OH• respectively. These will reduce and oxidize the organic contaminants completely to their respective products CO_2 and H_2O [22]. However, it exhibits faster recombination rate of the photo-generated electron-hole pairs than surface redox reactions. This seriously restricts the practical applications of ZnO especially in photocatalytic degradation of organic compounds.

Much research has been done in order to enhance its photocatalytic activity and this involves reducing the electron-hole pair recombination rate. This has been achieved by coupling the ZnO with other semiconductors or carbon based materials as well as doping with noble metals and non-metals [75]. This results in formation of hybrid materials that exhibit new functionalities which are valuable for several sectors such as in photocatalysis [50].

Romadhan etal [76] reported that, ZnO has been proven to exhibit antibacterial activity and has been greatly applied due to its low toxicity. This is also an advantage of employing ZnO nanoparticles in water treatment as it will also act against the bacteria in the water. This results in dye contamination free water as well as sterile water at the end of the process.

2.6.2 TiO_2 as a photocatalyst

Lately AOPs involving TiO_2have been greatly explored in the detoxification recalcitrant organic pollutants found in effluent water. It is the most widely studied catalyst due to its unique high photochemical reactivity, high photocatalytic activity, physical and chemical stability, low cost, availability, low environmental toxicity, electrical and optical properties [77]. $TiO_2$is a strong oxidizing material because of its semiconducting property that can be able to lower the activation energy for the degradation of organic pollutants. There are three different crystalline modifications of TiO_2 which are anatase, rutile and brookite. Anatase has been proven to exhibit the highest overall photocatalytic activity. The band gap energy of TiO_2 is 3.2 eV which is large. This means more energy is required to excite an electron and thus the higher the band gap energy the lower the photocatalytic activity. When a photon of energy equal to or greater than this band gap is absorbed, an electron is promoted from the valence band to the conduction band creating a hole or an electron vacancy in the valence band. However due to its large band gap, there is need

to reduce the energy by coupling with other semiconductors so as to expand its effectiveness in photocatalysis [78].

Activation of semiconductors is an exciting approach towards the photocatalytic degradation of organic pollutants. The band of TiO_2 results in low efficiency of the material and as well its individual use causes difficulties in the separation from the waste water after photocatalytic degradation which is difficult due to the small particle size. Therefore, there is great need to discover novel materials with high performance for use in heterogeneous catalysis. Prabhu et al [70] has reported on the degradation of rhodamine B by TiO_2-CeO_2-ZnO nanocomposite in aqueous solutions. Several researchers have reported on the combination of large band gap semiconductors like TiO_2 and ZnO with narrow bandgap conductors. This combination or coupling of these semiconductors result in the production of novel materials which can be used to solve water contamination problems using easy and less costly methods. Thus it is suitable to be applied in photocatalysis under UV irradiation for non-selective mineralization of hazardous organic pollutants found in effluent water [46].

2.6.3 $CoFe_2O_4$ and Spinel Ferrites

Recently studies on spinel ferrites have been extensively conducted. Spinel ferrites of Mg, Co, Ni and Zn have been shown to have excellent properties which include good magnetic performance, narrow band gap and excellent chemical stability [79]. These materials have been proven to show high adsorption capacities and surface area to volume ratio. The superparamagnetic properties of these nanoparticles have attracted great attention. Due to these special properties spinel ferrites have found great application in several fields which include the electronic industry, such as cores in high frequency inductors and transformers, microwave

devices, and television receivers. Generally, these applications require fine, uniform particles because they have high sintering activity and can give controlled microstructures [29], [65].

Based on their crystal structures and magnetic properties, ferrites are classified as spinel MFe_2O_4, where M is either Mn, Fe, Co, Ni, Co, Zn or garnet $M_3Fe_5O_{12}$ [30]. The cations of both positions are tetrahedrally and octahedrally coordinated to oxygen atoms, respectively. In the formula MFe_2O_4, depending on the position of M (II) and Fe (III) site preference, three possible spinel ferrite structures are known, namely normal, inverse and mixed [65]. Spinel ferrite materials are highly stable in both acidic and alkaline mediums. Thus they can be used throughout a broader pH range of 2-6. However, these ferrite nanoparticles exhibit limited photocatalytic performance due to their fast photo generated electron-hole recombination [32]. The application of cobalt ferrite and spinel ferrites in water treatment has been studied extensively. They have been coupled with other semiconductor materials that are capable of adsorbing or degrading organic contaminants. Spinel ferrites provide the ease of recovery of the material due to its magnetic property thus it makes the reuse of the material possible thereby reducing the capital investment [65].

Several [30], [31], [80] researches have been conducted in order to modify the surface of CoFe2O4. The modification of spinel ferrites is an approach done in order to overcome problems associated with the nanoparticles such as agglomeration, toxicity and leaching. This results in nano materials that have enhanced sorption capacities [79]. Spinel ferrites coated with silica exhibits increased stability in aqueous environments as well as increased biocompatibility. The surface of the coated ferrites is also further functionalized. This can be achieved by functionalizing the spinel ferrites with amino, anhydride and thiol groups [29].

2.7. Alginate in photocatalysis

2.7.0 Structure of Alginate

Alginate is made from algae and together with the algae-based polymers xanthan gum and carrageenan are used to improve the textures of foods such as chicken nuggets and ice cream. Alginate is a heteropolysaccharide composed of β-D-mannuronic acid and α-L-guluronic acid, widely distributes in diverse seaweeds and bacteria (Fig 2.1). It forms stable gels that could be cross-linked by various di/trivalent cations, such as $Ba^{2+,}$ $Ca^{2+,}$ and $Fe^{3+.}$ Alginate beads can be used to absorb hazardous waste from contaminated solutions, and beads are easy to collect and dispose [81].

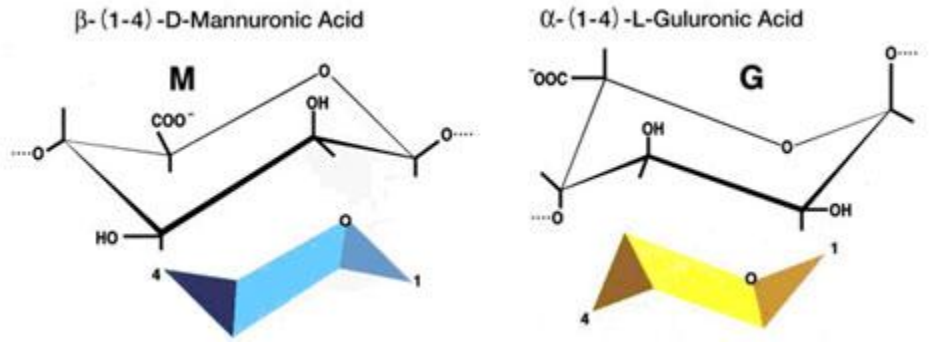

Figure 2.1 Structure of alginate.

2.7.1 Alginate and alginate beads in photocatalysis.

The implementation of heterogeneous photocatalysis has several limitations. The main problem associated with these processes is the difficulty in recovery and recycling of the photocatalysts after the waste water treatment process. Another issue is the leaching of the metal catalyst during the process of photocatalysis. These problems can be solved by the immobilization of the catalyst materials thus ZnO,TiO_2 and $CoFe_2O_3$ on a solid support material [36]. Therefore, it becomes a necessity to develop a less costly and environmental friendly entrapment technique

that can be used. According to Lewandowska [82], CaAlg is a non-toxic, biodegradable, non-immunogenic, water insoluble and thermally irreversible polymer type. CaAlg has been reported to prove better support for the immobilization of nanoparticles. CaAlg beads can therefore be used for the environmental friendly immobilization of catalysts and the photoactive beads used in water treatment.

Alginate is the salt of alginic acid and it is a natural polymer which is widely used as a component for entrapment. It is reported to be non-toxic, cheap, efficient, can be easily prepared and has an open lattice structure for the fast diffusion of dye molecules during adsorption. CaAlg has the ability to form stable hydrogels which can be used as a photocatalyst support. CaAlg can be modified so as to improve and enhance its chemical stability as well as adsorption capabilities [33]. Studies have shown that alginate can be modified by the use of crosslinking agents which reduce the particle size and increase the surface area and adsorption. Crosslinking agents that can be applied include $CaCl_2$ [37]. Recent word done has proven the feasibility of using CaAlg as the support material in the removal and degradation of dyes. A research by Ismail [83] has revealed that TiO_2 immobilized CaAlg beads have been investigated for the degradation of methylene blue dye and the recycled TiO_2-CaAlg beads were able to enhance the degradation process. This was due to the increased roughness of the beads as a result of the repeated usage. Another study has shown that the CaAlg polymer fibers have demonstrated high efficiency in the removal of MO from water. Researches proved that carbon based nanocomposite exhibited extraordinary adsorption efficiencies towards water treatment. The metal oxide catalysts were trapped in the alginate beads [34].

In photocatalytic degradation of organic pollutants, the carbon-based nanostructures act both as electron-acceptor and as electron-transport materials. The materials will also be facilitating the

migration of photo-generated electrons and slowing down the charge recombination and thus enhancing the lifetime of electron–hole pairs and improving the photocatalytic efficiency [40]. The ZnO, TiO_2 and $CoFe_2O_4$ nanoparticles have excellent photocatalytic activity that is more effective for the degradation of organic pollutants. The alginate beads on the other hand possess impressive adsorption ability for dyes and heavy metals due to the carboxylic groups which are more abundant in the alginate polymer [41]. The incorporation of these materials together can complement one another with their advantages and produce an effective material for the degradation of MO dye treatment [39].

2.8 Composites and their application in catalysis.

Several work has been done pertaining the application of composite materials. These have been proven to show many advantages over using individual catalysts. ZTC composite trapped in alginate beads has never been reported in literature. Many approaches have been done using composite materials in the efforts of enhancing the photocatalytic activity of the semiconductor materials. These techniques deal with the surface morphology control, noble metal loading and heterostructural modification[66], [84]. The mentioned approaches require complicated preparation procedures and hence simple and cheaper procedures should be invented. Nano composites are however known to have small filler size and distance between fillers thus high surface to volume ratio. Mechanical Properties are such as increased ductility with no decrease of strength, are obtained by synthesizing nanocomposites. Scratching resistance and improved optical properties is a light transmission characteristic that is particle size dependent [85].

2.9 Mechanism of photocatalysis

Photocatalysis depends on the wavelength or light energy and the catalyst involved. Generally semiconducting materials are employed as catalysts and they act as sensitizers for the irradiation of light stimulated redox process due to their electronic structure [27]. This ability of semiconductor catalysts to act as sensitizers consequently enhances the photocatalytic degradation of the MO dye. This is as a result of their electronic structure which is characterized by a filled valence band and an empty conduction band. Hence they are used in photocatalysis.

The semiconductor is illuminated with energy greater than the band gap and electron and holes pairs of excited high energy states are produced. Composites of ZnO/TiO_2favors the transfer of an electron from the conduction band of ZnO to the conduction band of TiO_2 upon light illumination and conversely the hole transfers from the valence band of TiO_2 to the valence band of ZnO consequently decreasing the pairs recombination rate. The lifetime of the charge carriers is hence increased effectively through this charge separation and the efficiency of the interfacial charge transfer to adsorbed substrates is enhanced [44].

2.9.1 Oxidation mechanism

The absorbed water on the surface of the photocatalyst is oxidized by the positive holes created in the valence band as a result of shift of electrons to the conduction bad. This shift of electrons is induced by the irradiation of light onto the photocatalyst [29]. This results in the formation of hydroxyl radicals (OH•). These radicals then react with organic compounds present in the dye molecules producing less harmful products which are CO_2 and H_2O. The presence of oxygen during this process gives rise to radical chain reactions of the intermediate radicals in the organic dye molecule and the oxygen is consumed. This results in the organic compounds being

degraded ultimately forming carbon dioxide and water. Under these conditions, the organic compounds undergo oxidative decomposition [27].

2.9.2 Reduction mechanism

This mechanism involves the reduction of oxygen absorbed from the air as a pairing reaction. This takes place as an alternative to hydrogen generation since oxygen is an easily reducible molecule. Electrons in the conduction band react with the dissolved oxygen to form superoxide anions. These anions attach to the intermediate products in the oxidative reaction, forming peroxide or transforming to hydrogen peroxide then water. This process takes place favorably in organic compounds than water. Hence the higher concentrations of the organic compounds increase the number of positive holes. This in turn reduces the carrier recombination and promotes photocatalysis [27].

2.9.3 Photocatalysis mechanism interferences

Effect of ionic salts

There are several species present in the real effluents which affect photocatalysis. These include organic and inorganic species and some examples of these are Cl^-, NO_3, SO_4^{2-}, CH_3COO^- and HPO_4^{2-}. The presence of these anions leads to an increase in the photocatalytic degradation. However, the presence of $HPO_4^{2-}$and CH_3COO^- anions decreases the photocatalytic efficiency. The presence of Cl^- anions on the oxidation process can be explained by the result of the reaction of photo produced OH• with Cl^- [44].

$OH\bullet + Cl^- \rightarrow OH^- + Cl\bullet$…… (1)

The Cl radicals are in principle also capable of oxidizing pollutants and to participate in the process of degradation. However, these Cl radicals can also react with organic compounds forming chlorinated organic compounds which are very toxic. CH_3COO^- reduces the photocatalytic degradation because it inhibits the formation of OH radicals on the surface of the catalyst as shown in the equations below.

$CH_3COO + hv \rightarrow CH_3 + CO_2^{+\bullet}$…… (2)

$h^+ + HO \rightarrow OH\bullet + H^{2+}$…… (3)

$h^+ + OH^- \rightarrow OH\bullet$…… (4)

The SO_4^{2-} ions also get adsorbed on the surface of TiO_2 and react with the photo induced holes forming the sulphate radial ion. This radical is a strong oxidant and engages in the three possible modes of reactions with organic compounds by abstracting a hydrogen atom from saturated carbon, addition to unsaturated or aromatic carbon and by removing one electron from the carboxylate anion and from certain neutral molecules [44].

2.10 Summary

To summarize, MO dye was defined as a toxic substance found in waste water and its presence in waste water even in minute concentrations poses a significant threat to human health. Removal of this dye from waste water is essential through waste water treatment to avoid the harms it causes. Conventional methods of methods of removal of this dye have been overridden by their disadvantages which have turned to be more significant than the advantages. These limitations vary from converting pollutants from one form to another, large band gap energies and difficulties in the recovery of the material from the treated water. The application of photocatalytic composites has proven to be successful and has value in the effective removal of

this toxic dye. Heterogeneous catalysis and nanocomposites have shown to be highly efficient, easy to use, easy to recover as well as effective reusability. Nanocomposites are defined by low band gap energy, low cost, effective conversion of pollutants to CO_2 and H_2O. Alginate has high carbon content and easy to convert into beads and this justifies the use of alginate based composites.

CHAPTER 3

METHODOLOGY

3.0 Introduction

This chapter focused on the procedures that were followed during addressing each and every objective of the study outlined in the first chapter. The procedures included synthesis of the nanoparticles, fabrication of the composite, characterization, mechanism investigation, recovery, reusability and stability studies of the composite.

3.1 Chemicals and equipment

All the reagents used were of analytical grade and were used as received. $Fe(NO_3)_3 \cdot 9H_2O$ TN, $CoCl_2 \cdot 6H_2O$ TN. NaOH (Fizmerk), Acetic acid (Glassworld), MO dye (Skylabs), $CaCl_2$ and Zinc

Acetate (Sigma-Aldridge, Germany), Ascorbic acid (ACE), EDTA (ACE), Ethanol (Glassworld), Alginic acid sodium salt (Sigma-Aldridge, UK).

3.2 Synthesis of ZnO nanoparticles

Zinc acetate dihydrate(12.0011g) was dissolved in 100 mL of deionized water in a 250 mL conical flask through continuous magnetic stirring. In a separate beaker, a 0.8 M NaOH solution was prepared by dissolving 3.2034 g in 100 mL of deionized water. NaOH (0.8 M) solution was transferred to the zinc acetate dihydrate solution in a drop wise manner under magnetic stirring to a final pH of 9 at a temperature of 60 ^{0}C and was stirred for 3hs. The suspension formed was left to age overnight. The precipitate was centrifuged at 3000rpm, washed twice with distilled water, dried at 80 ^{0}C for 12h and was calcined at 550 ^{0}C for 4h [64].

3.3 Synthesis of $CoFe_2O_4$

$CoCl_2.6H_2O$ (1.1901 g) was dissolved in 500 mL distilled water in a 1000 mL conical flask and $Fe(NO_3)_3.9H_2O$ (4.0408 g) was dissolved in 500mL in separate beaker. The two solutions were mixed using magnetic stirrer and CTAB was added. The mixture was heated to 80 ^{0}C under magnetic stirring for 2h. NaOH was added until a pH of 10.5 was reached and was maintained for 3h. The sample was left to age for 4h. The suspension was washed 3 times with ethanol: water (1:1) and centrifuged at 500rpm at 5 ^{0}C for 10 min. The solid product was dried in an oven at 80 ^{0}C for 12h. The final sample was calcined at 600 ^{0}C for 2h [80].

3.4 Fabrication of the $ZnO/TiO_2/CoFe_2O_4$ nanocomposite trapped in alginate beads

The composite was fabricated via immobilization of the nanoparticles in calcium alginate beads. This was achieved by dissolving 4.383 g of alginate in 500 mL of water and was magnetically

stirred at room temperature overnight. A portion of the alginate solution was dropped into a 100 mL solution of 2% $CaCl_2$ and beads were instantly formed. The beads were isolated, dried at 60 ^{0}C for 24h. Masses of (0.25 g) ZnO, (0.25 g) TiO_2 and (1 g) $CoFe_2O_4$ were weighed, dispersed into 25 mL of water and sonicated to homogeneity. The nanoparticle suspension was then transferred to the alginate solution, sonicated then stirred to homogeneity using a magnetic stirrer. The homogeneous alginate-photocatalysts composite suspension was then placed into a burette and set to drop into 200 mL of 2% $CaCl_2$ solution. The beads formed were then added to 100 mL of 5% $CaCl_2$ solution and left under continuous gentle magnetic stirring for 3h in order to harden them. Fabrication of the second and the third composites were done in the same manner. The beads were then isolated from the excess $CaCl_2$ by decanting and were washed 3 times with distilled water then dried at 60^{0}C for 24h [88].

3.5 Characterization of the nanocomposite

The composite and individual catalysts were characterized by Fourier Transform Infrared (FTIR): Nicolet 6700 Thermoscientific, Thermogravimetric Analysis (TGA): TGA 550 Advanced laboratory solutions, X-Ray Diffraction (XRD), Transmission Electron Microscopy and Selected Area Electron Diffraction (SAED)

3.5.1 FTIR

The individual photocatalysts, ZnO, TiO_2, $CoFe_2O_4$, alginate beads and the ZTC composite were analyzed to identify the functional groups present on their surfaces. The materials along with NaCl were weighed in the ratio 1: 100 respectively. The mixture was homogenized by means of grinding using mortar and pestle then pressed into a sample holder and placed into the FTIR spectrometer. The sample was scanned from 400 cm^{-1} to 4000 cm^{-1} at an interval of 4 cm^{-1} [89].

3.5.2 TGA

TGA analysis of the ZnO, TiO_2 and $CoFe_2O_4$, alginate beads and the ZTC composite catalyst was done under a N_2, ramping the temperature from 25-800^{0}C at 10 ^{0}C per minute. Masses of 5 mg were used on all the samples under analysis [90].

3.5.3 XRD

The samples were ground to a talc like powder (<0.062mm) and placed in the center of a quartz disk. Two –three drops of acetone or water were added to the sample and was spread to a thin layer with a glass rod. The samples were then placed in a desiccator to dry and scanned on the XRD scanning from 20 to 90 2Ɵ (theta) degrees [91].

3.5.4 TEM

To image the nanoparticles and the ZTC composite on the TEM, finely ground beads samples were dispersed in 1 ml of ethanol and then they sonicated for 30-40 minutes to get a solution of magnetic nanoparticles. Approximately 10–20 μL of this solution was dropped onto a 3 mm copper grid, which was then dried at room temperature. Finally, the copper grid was inserted into the transmission electron microscope [91].

3.6 Investigation of photocatalysis

Photocatalytic degradation of MO dye was investigated under the following parameters: the effect of pH which ranged from 6-10, initial dye concentration of the range 1-100 mg/L, contact time of the range 30-300 min and the catalyst dosage of the range 0.05-1 g on the rate of MO degradation. The experiments were done in duplicate analysis and a constant volume of 20 mL was used. Two control samples were included in every experimental set up which were one with

the dye solution and the composite kept in the dark (adsorption control) as well as the one with the dye solution only exposed to sun light (photodegradation control). Ambient temperature and the stirring rate of 100 rpm remained constant throughout the experiments. The mechanism of photocatalysis, stability studies, recovery and reuse of the composite was investigated.

3.6.1 Effect of precursor catalyst ratio on the degradation of MO

UV/Vis spectrophotometer was calibrated using a series of standard solutions of MO. The standards were prepared from serial dilutions of a 10 mg/L solution which was made by dissolving 10 mg in 1 L of distilled water. Dilutions were made and solutions of concentrations: 1, 2, 4, 6, 8 and 10 mg/L were obtained. The standard solutions were run on the UV/Vis: 2000 Series Digilab, Merlin USA at 464 nm and a standard calibration curve was obtained [92]. A pre-run of the photocatalytic experiments was performed using the fabricated composites. Each of the ZTC composites, (0.15 g) in 20 mL of a 10 mg/L MO solution, pH 7.5, 30 minutes' adsorption/desorption time and 5 hours' exposure time was used. Two control samples were used which contained the same concentration of the dye and one had no composite which was exposed to light and the other had the composite but was left in the dark during the photocatalysis of the other setups. The samples were placed in beakers and exposed to sun light for 5 hours. Solution samples were analyzed using the UV/Vis spectrometer for the initial and final absorbance. The best catalyst was used in further optimization studies [93].

3.6.2 Effect of pH on the degradation of MO

The effect of pH was established by running photocatalytic degradation experiments varying the pH of the MO solution from 6-10. This pH range was used because MO is highly sensitive to pH and exhibits the MO traits around the neutral pH. The pH values of the MO solution were

adjusted by 1 mg/L of HCl and 1 mg/L of NaOH. A mass of 0.15 g of the first ZTC composite was transferred to 20 mL of 10 mg/L MO dye into a beaker. Duplicate analysis was done, adsorption/desorption time was 30 minutes and the photocatalytic degradation was run for 5 hours [93]. After 5 hours of exposing the samples to sunlight, samples were centrifuged and analyzed using the UV/Vis spectrometer.

3.6.3Effect of initial concentration of the MO on degradation

The effect of initial dye concentration was investigated by varying dye concentrations in photo degradation studies. Duplicate analysis was done on all the concentrations and the catalyst dosage for all the experiments was 0.15 g, predetermined optimum pH of 8 was used and the contact time was 5 h. The initial dye concentration was varied from 1, 5, 10, 15, 20, 25 and 100 mg/L. Samples were left in the dark for 30 minutes prior to sunlight exposure. After 5 h of exposing the samples to sunlight samples were collected, centrifuged and analyzed using the UV/Vis spectrophotometer [93].

3.6.4Effect of contact time on the degradation of MO dye

The effect of contact time was investigated by performing several experiments varying the contact time of the catalyst, the dye solution and the light exposure. The mass of the ZTC composite catalyst used was 0.15 g, pH 8 and the predetermined effective initial concentration of the dye solution of 10 mg/L was used. The MO solution volume used was 20 mL and duplicate analysis was done on the samples. The samples were left in the dark for about 30 min to attain the adsorption/desorption equilibrium and were then exposed to solar lighting varying the time of exposure. Aliquots were collected during the course of the experiment at time intervals that is 0, 30, 60, 90, 120, 150, 180, 220, 250, 280 and 300 min. The aliquots collected were analyzed by

the UV/Vis spectrophotometer and returned to the beakers before the experiment was resumed [27].

3.6.5 Effect of catalyst dosage on the degradation of MO dye

The effect of catalyst amount added to the dye solution was investigated by varying the mass of catalyst added for the photocatalytic degradation studies. MO, 20 mL of 10 mg/L dye concentration, pH 8 and 3 h exposure time which were the predetermined optimum conditions for the degradation. The experiments were run in duplicate analysis. The catalyst dosage was varied from 0.05, 0.1, 0.15, 0.2, 0.25 0.3, 0.5 and 1 g and the samples were left in the dark for 30 min then exposed to sunlight [93]. After 3 h of sample exposure to sunlight, the samples were centrifuged and analyzed using the UV/Vis spectrometer.

3.7 Mechanism investigation

To determine the possible mechanism of degradation of MO by the ZTC composite trapped in porous carbon spheres, several scavengers were used in order to quench relevant active species. The predetermined pH, initial concentration, time and catalyst dosage were used in the experiments. Ascorbic acid (AA), EDTA, Cupric nitrate and ethanol were used to be the scavengers of the superoxide radical ($O_2^{\bullet}$), holes (h+), electrons (e^-) and the hydroxyl radicals ($OH^{\bullet}$) respectively. Each scavenger, 5 mL of 0.5 M was added to 20 mL of 10 mg/L, pH 8, 0.15 g of the ZTC composite and samples were left in the dark for 30 min to attain adsorption/desorption equilibration prior to exposure to the sun light for 4 h. After exposure, the samples were centrifuged and analyzed using the UV/Vis Spectrophotometer and the differences in the degradation was used to deduce the possible mechanism [94].

3.8 Recovery and reusability studies of the composite

A piece of magnet was placed outside the beaker and the solution was decanted. The catalyst was washed three times with distilled water and then dried at 60 ^{0}C for 24 h. The catalysts were reused in other photocatalytic experiments and the rate of degradation was monitored[32]. The catalysts were rigorously washed with distilled water, dried and FTIR characterization was done.

3.9 Stability studies of the composite

Stability studies were done by on catalysts that were used in the previous experiments several times. Metal analysis was done on the solutions by analyzing the solutions using Atomic Absorption Spectrometry (AAS). The recycled sample, a fresh sample of the ZTC composite and the alginate beads were weighed, 0.5 g of each sample. The samples were weighed into porcelain crucibles and placed in a muffle furnace at 800 ^{0}C. After 30 min, the samples were removed from the furnace, reweighed and placed in 50 mL beakers. Aqua regia, 10 mL was added to each of the samples and was placed on a hot plate for 10 min. After cooling, the solutions were transferred to 50 ml volumetric flasks and were topped to the mark using distilled water. The solution samples were analyzed using the AAS and the amount of zinc, iron and cobalt was determined [95].

CHAPTER 4

RESULTS AND DISCUSSION

4.0 Introduction

This chapter serves to present results of the experimental findings of the afore mentioned methology, both statistical and raw data are presented in greater detail in line with the set aims and objectives of this research. The results obtained are presented in form of spectra, graphs and tables.

4.1 FTIR Results

Fig 4.0 shows the FTIR spectra of the individual nanoparticles of ZnO, TiO_2 $CoFe_2O_4$, the alginate beads and the synthesized ZTC composite acquired in the range 4000-400 cm^{-1}.

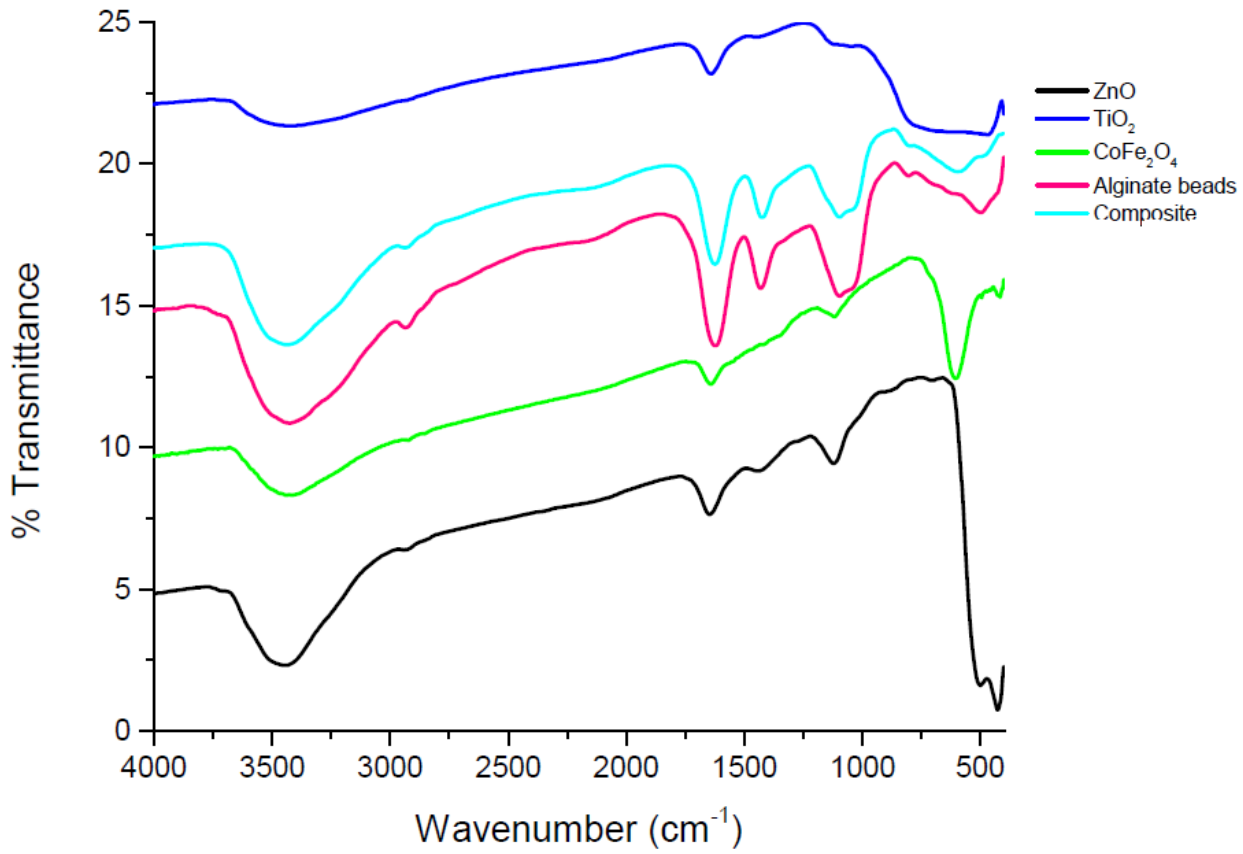

Figure 4.0: FTIR Spectra of the nanoparticles, alginate beads and the ZTC composite

The spectra of the ZnO nanoparticles synthesized from zinc acetate and NaOH at pH 9 shows a vibrational frequency at 3143 which corresponds to the O-H vibrational frequency which is as a result of the NaOH added to the solution during the synthesis. The O-H bending mode of vibration found at 1647 and 1433 cm^{-1} represents the hydroxyl groups indicative of the water molecules absorbed from the atmosphere [96]. ZnO corresponds to the peak at around 530 cm^{-1} which indicate the formation of the ZnO. According to previous researchers, the ZnO peak that appears in the range 550-453 cm^{-1} represents the complete formation of ZnO [97]. The spectra in Fig 4.0 representing the synthesized $CoFe_2O_4$ powders shows a vibrational band at 3433 cm^{-1} represents the O-H groups which are as a result of both the absorbed and free water in the sample. Strong vibrational frequencies at found at 608 and 429 cm^{-1} exhibit the formation of single phase spinel structure [31]. Strong absorption frequencies are indicated in the region 400-

800 cm^{-1}in the spectrum of TiO_2 in Fig 4.1 and this corresponds to the Ti-O-Ti bonding which indicates the formation of a titanium oxide. This spectrum clearly shows that the TiO_2 as indicated by Liu et al [98] that absorption peaks in the range 426-663 cm^{-1} shows the characteristic of the TiO_2.

The spectrum of calcium alginate in Fig 4.0 shows a broad peak at 3422 cm^{-1}which is attributed to the hydroxyl groups and a little change in its peak position and intensity was observed after the addition of the nanoparticles, Dong et al [98]. However, this cannot be used as evidence for the incorporation of the nanoparticles into the alginate matrix. The stretch vibration at band at 2932 cm^{-1} is assigned to the stretch vibration absorption of C-H from glucose units in alginate chains. The corresponding band becomes very weak in the spectrum of the ZTC composite beads. Two bands at 1623 cm^{-1} and 1431 cm^{-1} are assigned to the asymmetric and symmetric stretching vibrations of the carboxyl group (C–O–O) of alginate molecule, respectively [35]. There was no significant shift in their positions and intensity. An additional sharp peak at 1096 cm^{-1} is for the C–O groups in the alginate, but a change in its shape and position is not found in the gel beads [81].The vibrational band at 499 cm^{-1} the alginate is attributed to the Ca in the beads, crosslinking the alginate molecules. This band is only shifted in position but no significant change is observed in its intensity in the ZTC composite. This shift is due to the presence of the nanoparticles which are metal oxides. This shift is as a result of a combination of frequencies from metals.

4.2 TGA analysis of the nanoparticles and the composite

Thermogravimetric analysis was used to study the behaviour of the as-prepared samples in a nitrogen atmosphere from 25 to 800 ^0C, ramping the temperature at 10 $^0C\ min^{-1}$. As indicated in the Fig 4.1 below, the thermograms for all the nanoparticles showed similar trends.

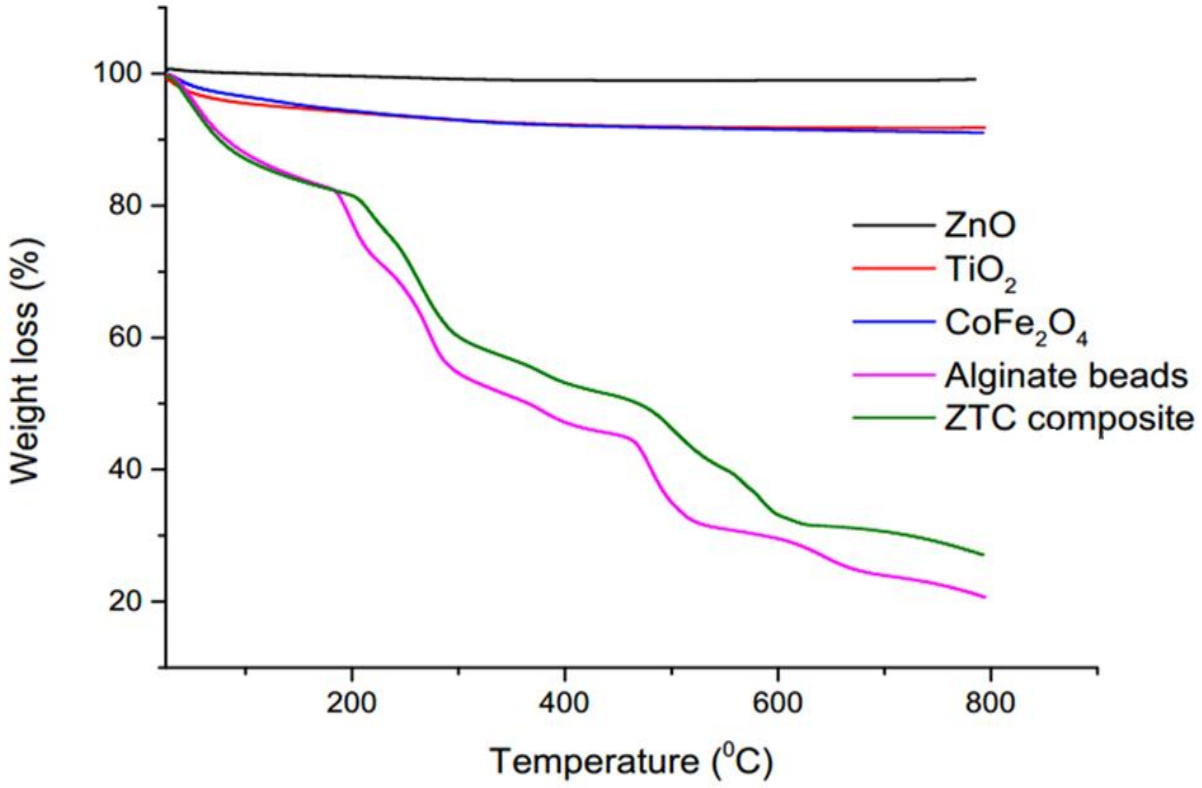

Figure 4.1 TGA Results of the nanoparticles, alginate beads and the ZTC composite

With increase in temperature, ZnO nanoparticles had a weight percentage decrease of about 1% up to 300 ^{0}C. $CoFe_2O_3$ and TiO_2 also had a similar weight loss of 8% up to a temperature of 400 ^{0}C. This weight loss is attributed to the loss of water absorbed by the nanoparticles and some volatile compounds absorbed on the surface of the particles. This small weight loss indicates that the nanoparticles are thermally stable and they do not decompose [49], [85], [98]. On the other hand, the thermograms for calcium alginate beads and the ZTC composite also showed similar trends. The calcium alginate beads thermogram, there were two significant weight loss phases. The first loss may have been due to the presence of water in the sample. This takes place slowly up to a temperature of 200 ^{0}C, and a rapid weight loss from a temperature of 200-300 ^{0}C. Saravanan et al mentioned that this weight loss can be as a result of breaking of the alginate backbone into stable intermediates and loss of abundant hydroxyl groups on the calcium alginate

beads in the form of water. At higher temperature, calcium alginate will undergo decarboxylation forming CO_2. This takes place slowly in the temperature range of 450-550 ^{0}C due to the nitrogen environment and the final weight loss was about 80% [23].

Calcium alginate was not completely degraded in the temperature range of 500-800 ^{0}C. A weight of over 20% was maintained and this is similar to the results produced by Dong et al [35]. However, it was noticed that there was a slight shift in the weight loss of the ZTC composite and it was lower than that of calcium alginate. The weight loss of the composite was within the temperature of 350 ^{0}C and this indicates that it has a greater heat stability compared with the calcium alginate in this temperature range. This may imply that the metals cross-linked with the carboxyl groups in the alginate chains to form metal-alginate complexes, Fajriyati et al [49]. A 30% weight was maintained in the ZTC composite which is much higher than that of alginate beads only. This is an indication that the ZTC composite has an enhanced thermal stability than the calcium alginate alone. The difference between the two graphs, alginate beads and the composite is the percentage of the nanoparticles in the nano-composite [23]. This percentage was 10% of the whole mass of the composite.

4.3 TEM and SAED results for ZnO

The fine powder of ZnO nanocrystals was analyzed using the high resolution transmission electron microscope (HRTEM). The image obtained is shown in Fig 4.2 below which shows the crystallinity of the particles.

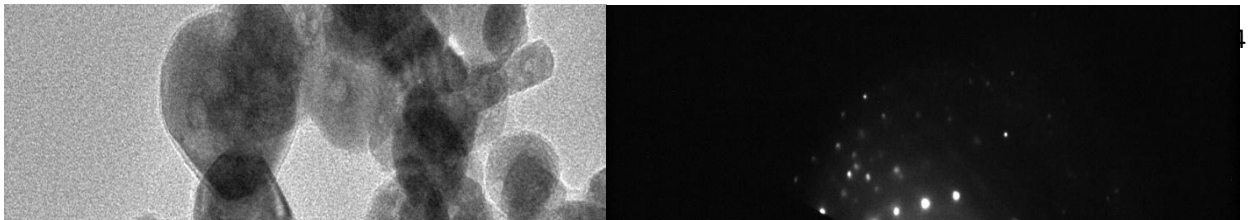

Figure 4.2 TEM & SAED images of ZnO

The particles show that their size is in the nano-region. This confirms the synthesis of the ZnO nanoparticles. The SAED shown above supports the crystalline structure of the nanoparticles. These pictures substantiate the approximate spherical shape of the nanoparticles, and most of the particles exhibit some faceting. From the pictures, it also can be seen that the size of the nanoparticle is less than 100 nm which confirms the formation of nano-sized particles [99]. The selected area electron diffraction (SAED) pattern (Figure 4.2) shows distinct bright rings which confirm the preferential orientation of nanocrystals instead of irregular [100]. Transmission electron microscopic pictures have also revealed the ZnO nanoparticles formation by confirming the hexagonal plane to the prepared nanoparticles [21].

4.4 TEM and SAED results for $CoFe_2O_4$

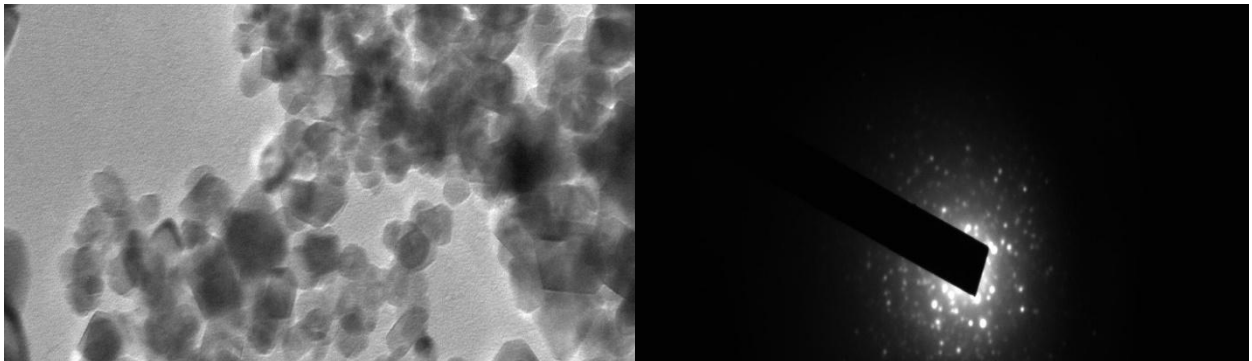

Figure 4.3 TEM & SAED images of $CoFe_2O_4$

The TEM and SAED images of cobalt ferrite samples are shown in Fig 4.3. The results indicate that the synthesized sample are uniform in both morphology and particle size distribution. Most of the particles appear spherical in shape however, some elongated particles are present. Some moderately agglomerated particles as well as separated particles are present in the images [30], [31]. All the particles were below 100 nm in diameter and this confirms the formation of nanoparticles. The SAED image shows the crystalline structure of the $CoFe_2O_4$. This is indicated by the reflectance of light by the crystalline particles [101].

4.5 XRD results for the nanoparticles and the composite

The morphologies of the synthesized particles are shown by the patterns in Fig 4.4. The spectra patterns for ZnO are in accord with the typical ZnO structure.

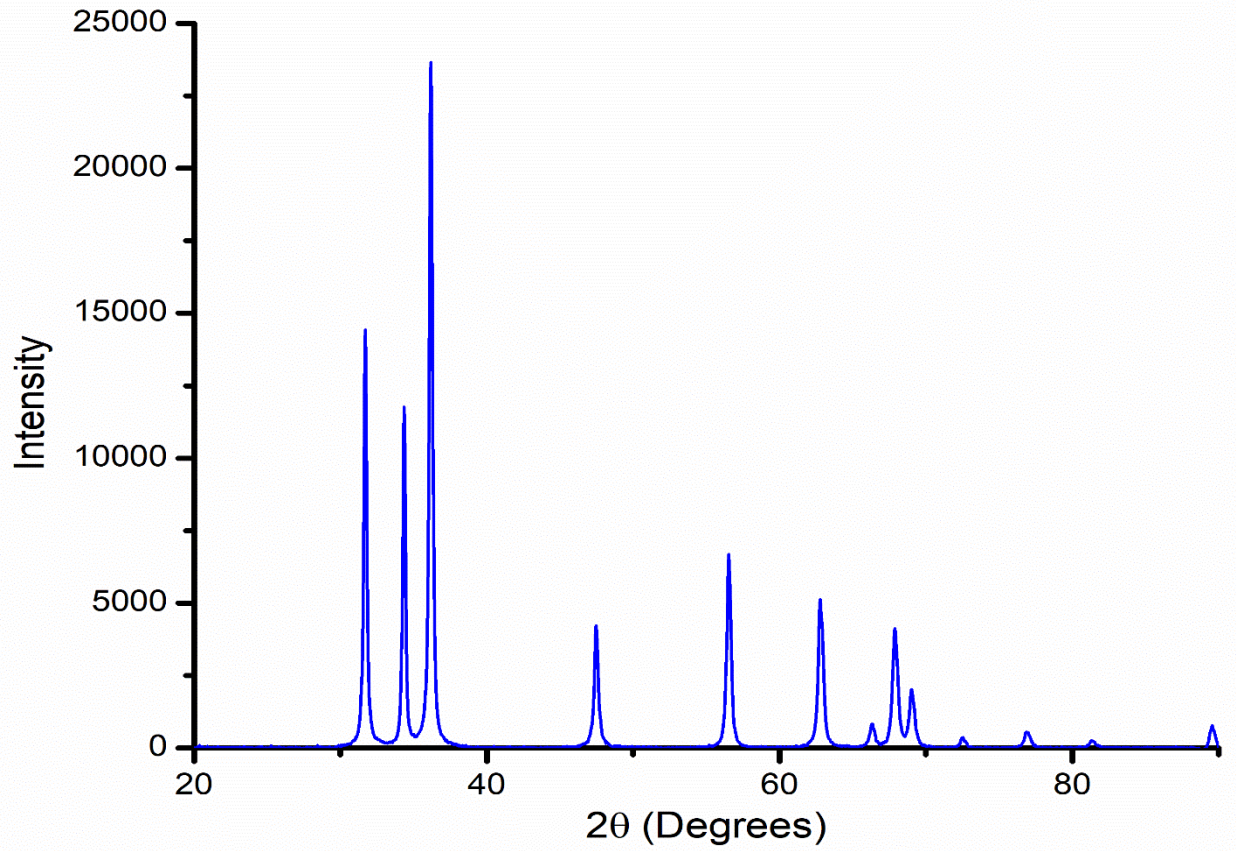

Figure 4.4 XRD spectrum of ZnO nanoparticles

The sharpness, strong intensity and narrow width of ZnO diffraction peaks in the XRD pattern indicate that the particles were crystalline [73]. A definite line broadening of the XRD peaks indicates that the prepared material consists of particles in nanoscale range. From this XRD patterns analysis, the peak intensity, position and width was determined. The diffraction peaks located at 31.84°, 34.52°, 36.33°, 47.63°, 56.71°, 62.96°, 68.13°, and 69.18° have been keenly indexed as hexagonal wurtzite phase of ZnO [76]. Furthermore, it also confirms the synthesized nanopowders were free of impurities as it does not exhibit any characteristic XRD peaks other than ZnO peaks.

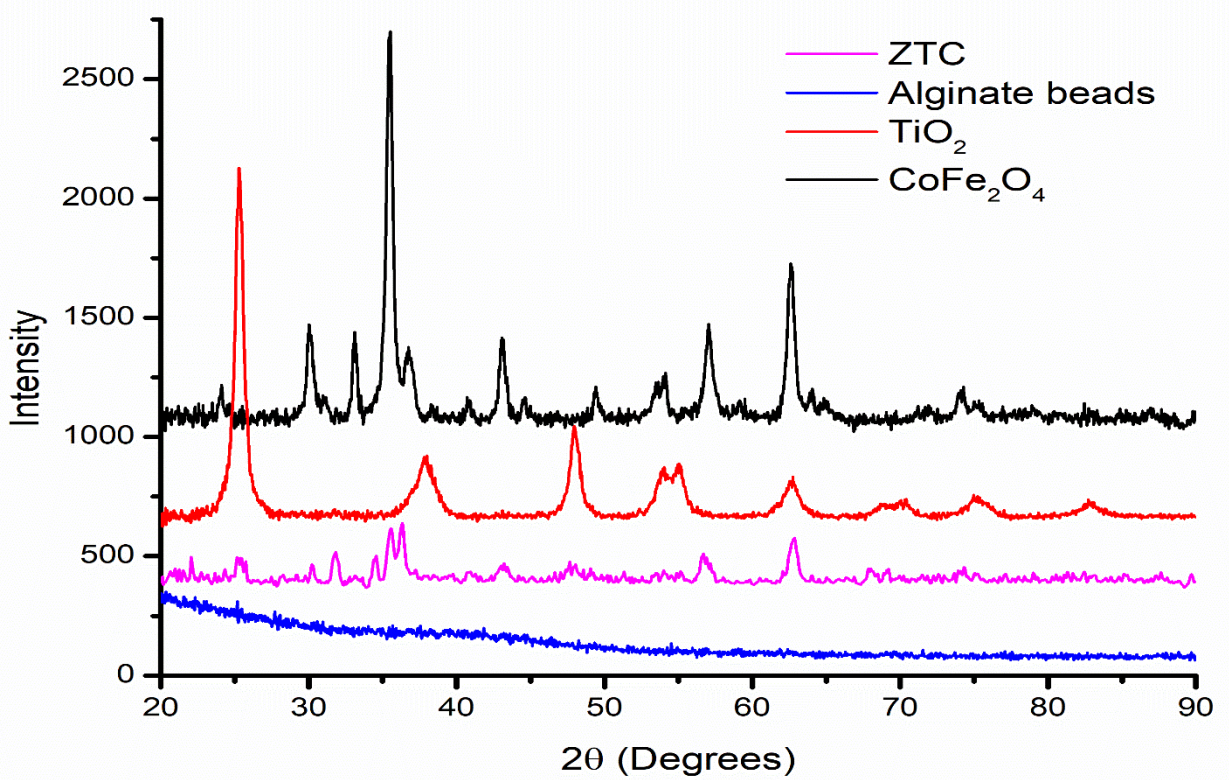

Figure 4.5 XRD spectra of the nanoparticles and the composite

Cobalt ferrite nanoparticles were prepared by co-precipitation method. Phase purity and nanocrystalline nature of the prepared sample was confirmed by the XRD spectrum. There are no other peaks showing in the spectrum representing the presence of cobalt oxide and iron oxide [30]. The XRD pattern of the commercial titania nanoparticles is shown in Fig 4.4. Liu et al. reports that absence of spurious diffractions indicates the crystallographic purity [98]. The experimental XRD pattern agrees with the XRD pattern of TiO_2 nanoparticles in other [26]. The 2θ at peak 25.4° confirms the TiO2 anatase structure. Strong diffraction peaks at 25° and 48° indicating TiO2 in the anatase phase [50]. There is no any spurious diffraction peak found in the sample. The 2θ peaks at 25.27° and 48.01° confirm its anatase structure. The intensity of XRD peaks of the sample reflects that the formed nanoparticles are crystalline and broad diffraction peaks indicate very small size crystallite [25]. It can be clearly seen that all of ZnO-based

materials revealed semblable diffraction peaks. Some of the 2θ peaks observed were corresponding to the hexagonal wurtzite structure ZnO [100]. The weaker the diffraction peak intensity of 26.0◦ corresponded to the amorphous alginate carbon backbone. Moreover, no obvious diffraction peaks of anatase TiO2 were observed which was attributed to the stronger peak intensity of ZnO [35].

4.6 Effect of pH on the degradation of MO

Effluent water to be treated using this method can be found at different pH levels. The study of the effect of pH on the degradation of MO dye is important towards the application of the composite. It is one of the most influencing factors on the rate of degradation. The pH from 6 to 10, using a concentration of 10 mg/L for 5 hours is shown in Figure 4.2 below.

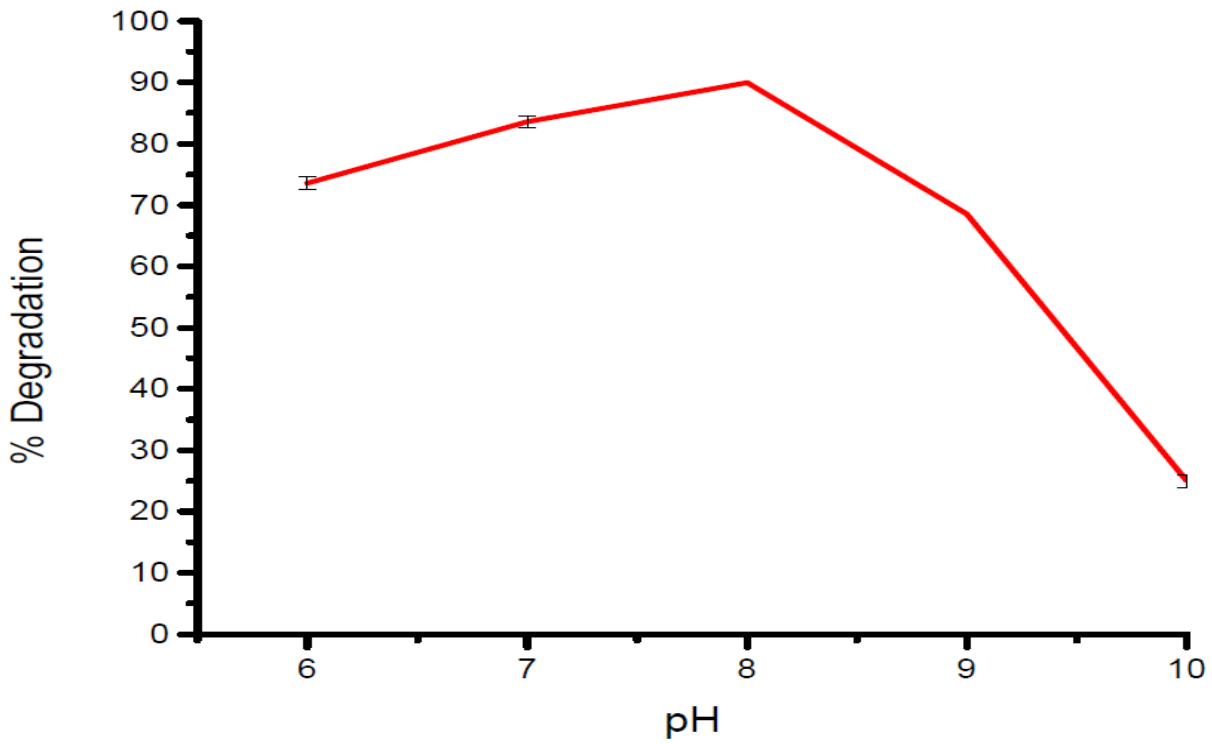

Figure 4.6 Effect of pH on the rate of photocatalytic degradation of MO

The best pH that exhibited the highest degradation was in the alkaline region of pH 8. However, there was a small difference in the influence of pH. With an increase in the pH of the solution the decrease in the rate of degradation may be attributed to excess OH^- which gives rise to quenchers hence colliding with the reactive species thereby reducing the rate of degradation. This range of pH was used as a result of the behaviour of MO under different pH conditions. Under acidic conditions, MO is reported to exhibit a red color. This results in the distortion of the absorption wavelength. Therefore, the pH conditions used were ranging from less acidic to basic. Additionally, at very basic conditions, that is pH above 10 MO dye tends to exhibit a yellow color and also the wavelength of absorption changes. This results in distortion of results as this solution absorbs more on a different wavelength from MO in the less acidic and less basic pH conditions [50].

The other factor that influenced the choice of the pH conditions is that the composite contains ZnO nanoparticles. These are sensitive to pH and is soluble in acidic solutions. Acidic conditions favor the hydrolysis of the ZnO nanoparticles. At low pH levels ZnO is undergoes dissolution and ZnOH is formed which could leach out of the composite [102]. As shown in the graph, the rate of degradation increases with increase in the pH. The results in the graph shows that the rate of degradation is much higher at neutral pH conditions and the highest degradation was experienced at pH 8 [103]. This is due to the facilitation of the formation of OH^- ions by the alkaline medium and these ions are responsible for the generation of the $OH^\bullet$ radicals which leads to an increase in the rate of photocatalytic degradation of MO. However, the decrease in the rate of degradation at pH 9 and 10 can be attributed to the dissolution of ZnO hence the optimum pH was found to be 8 [5]. Another important factor is the surface charge of the photocatalysts, the size of aggregates formed, the charge of the dye molecules, the adsorption

onto the catalyst surface is influenced by the pH as well. Since MO is an anionic dye, its adsorption and photocatalytic activity is related to the pH. As the photocatalytic reactions occur at or near the surface of the photocatalysts, it is believed that a phenomenon takes place, preventing surface contact, such as a boundary layer diffusion resistance or an electrostatic repulsion, which has a tendency to reduce the photocatalytic degradation [104].

4.7 Effect of initial dye concentration on the rate of MO degradation

Fig 4.7 Effect of the initial dye concentration on the rate of photocatalytic degradation of MO

The effect of initial MO concentration on the photocatalytic degradation was studied by varying the concentration of MO from 1- 100 mg/L, at a constant catalyst loading of 0.15 g/ 20 mL for 5 hours.

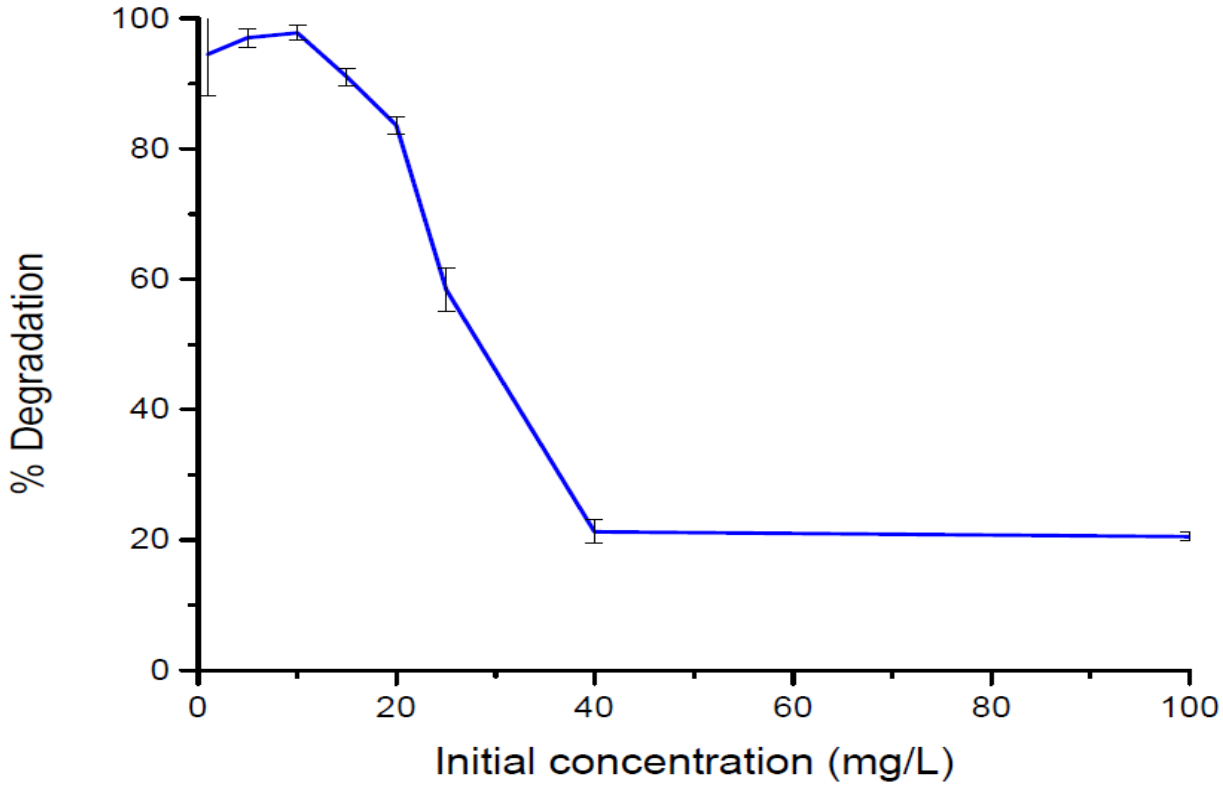

Figure 4.7 Effect of the initial concentration of the dye on the rate of degradation of MO

It was discovered that degradation the percentage is strongly influenced by the initial dye concentration and decreased from 100% to 32% with increase in concentration of dye from 1 mg/L to 100 mg/L (Fig.4.7). The optimum initial dye concentration was found to be 10 mg/L because it is the highest concentration that was completely degraded by the catalyst. The rate of degradation is related to the available catalyst surface for the generation of electron-hole pair, which in turn generates hydroxyl radicals. In this case, the amount of catalyst is kept constant and thus number of hydroxyl radicals generated remains same, while dye concentration is increased. Thus the number of hydroxyl radical which attack dye molecule decreases and thus rate of degradation decreases. Upon the increase of the initial MO concentration, the dye molecules accumulate on the surface of the ZTC composite catalyst. Quenching between these excited MO dye molecules irradiated by visible light takes place. The quenching probability could also increase with the increase in the initial concentration of the MO [47], [56]. Consequently, the photocatalytic degradation efficiency of the MO solutions decreases with an increase in the initial concentration as shown in Fig 4.7 above.

4.8 Effect of exposure time on the degradation of MO

The effect of exposure time was varied starting from 30 min to 300 min. The other parameters used were the predetermined optimum conditions and were kept constant throughout the experiment. Aliquot samples were collected after every 30 min and they were centrifuged, analysed and replaced back into the reaction beaker before the experiment was resumed. The results obtained are shown in the Fig 4.8 below.

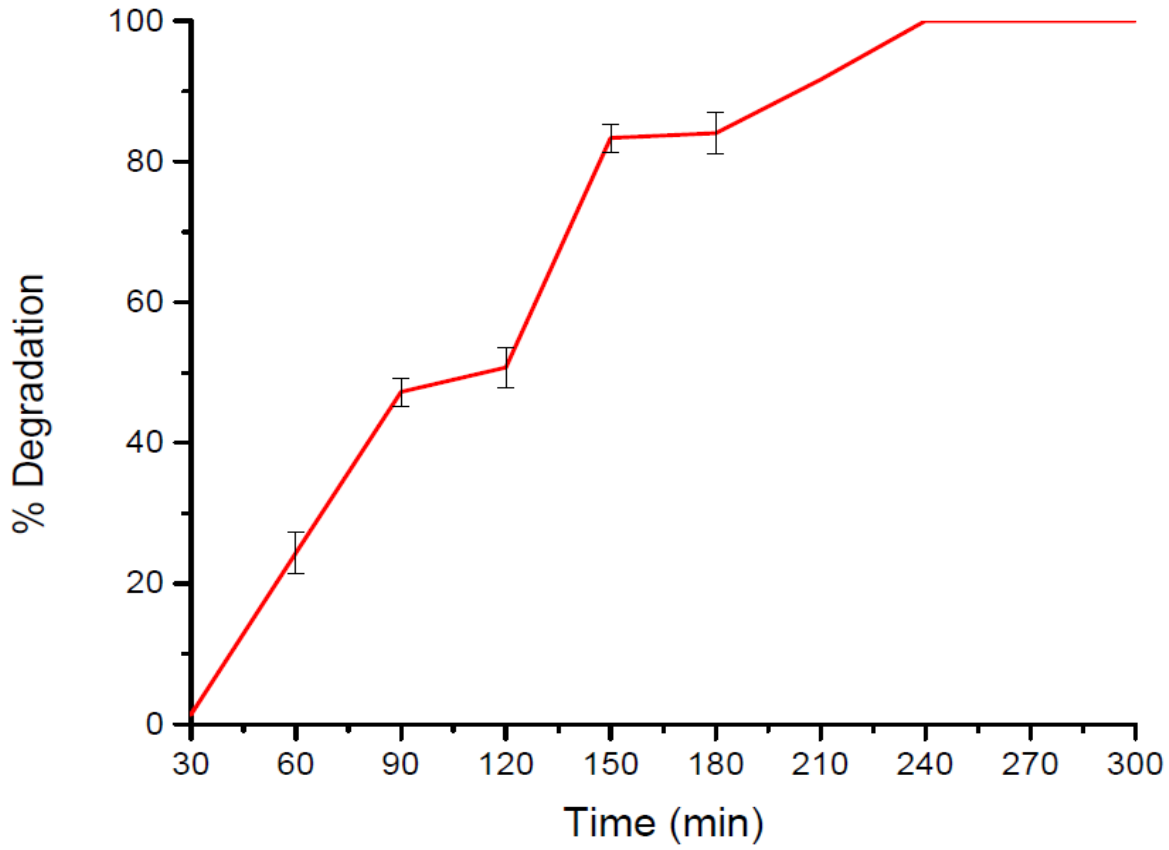

Figure 4.8 Effect of exposure time on the rate of MO photocatalytic degradation.

The effect of exposure time indicated that there was a rapid increase in the degradation of MO dye during the first 60 min of exposure to the sun. this is as a result of the less substrate and less intermediates which may cause interference on the catalyst. The degradation continues to increase and after 250 min, a degradation percentage of 100% was achieved due to more time of particle collision between the dye and the OH radicals [13]. This proves that as the time of exposure is increased, the degradation increased until 250 min which is the optimum time that the catalyst needs to completely degrade MO dye as shown in Fig 4.8 above.

4.9 Effect of catalyst dosage on the degradation of MO

One of the main parameter for the degradation of MO in photocatalysis is the catalyst dosage. The effect of catalyst dosage on the photocatalytic degradation of MO dye, experiments were carried out by varying the amount of the ZTC composite catalyst added to the dye solution. Other parameters were kept constant throughout the experiments. These include the pH 8, initial dye concentration 20 mL of 10 mg/L, and the solutions were exposed to the sun light for 5 hours at constant stirring.

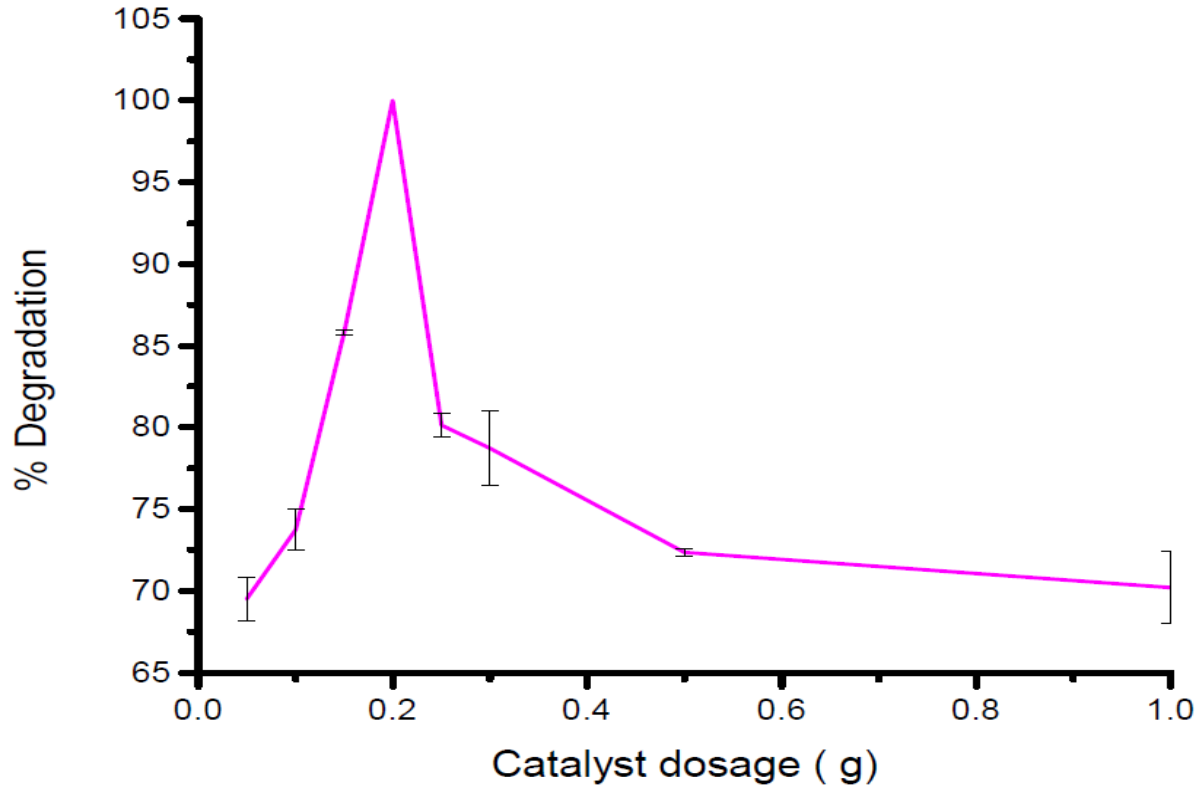

Figure 4.9 Effect of catalyst dosage on the rate of photocatalytic degradation of MO

The effect of an increase in the catalyst dosage is shown in Fig 4.8 above. It was observed that the concentration of MO dye decreased. The rate of degradation increased by the increase in the concentration of the catalyst from 0.1-0.2 g. This was probably due to the increase of the active sites as the amount of the catalyst increases. Therefore, there was a sharp increase on the

degradation of MO from 0.05-0.2 g/. The lower rate of the degradation at lower catalyst concentration is due to the light energy illuminated but lesser energy is used as less sites are available for excitation of electrons [56], [104]. On the other hand, a further increase in the catalyst dosage beyond the optimum concentration, degradation is reduced. This is due to the decrease in the opacity of the solution thereby increasing light scattering and infiltration depth of photons. Also agglomeration of the catalysts reduces photocatalysis hence reducing the surface active sites as well as deactivation of activated molecules could results in collision of intermediates [21].

4.10 Photocatalytic degradation under optimum conditions

Runs	% Degradation
1	98.57
2	97
3	99.7

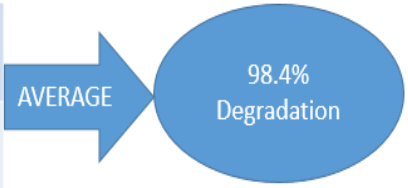

Figure 4.10 Photocatalytic degradation under optimum conditions

Photocatalytic degradation of MO was carried out under optimum conditions which were pH 8, 10 mg/L, exposed for 250 min at a catalyst dosage of 0.2 g. triplicate analysis was done and the dye volume was 20 mL, temperature and stirring rate was kept constant. The results shown below were obtained with an average degradation of 99%. This shows that the factors used were optimum for the degradation of MO dye using ZTC composite.

4.11 Investigation of the mechanism of photocatalytic degradation of MO dye

Investigation of the mechanism was done using several scavengers. The scavengers were added to the photocatalysis beakers at a constant concentration. To probe the role of hydroxyl radicals, ethanol was added. Ethanol react rapidly with hydroxyl radicals and have been extensively used as $OH^{\bullet}$ scavengers to determine the presence and role of hydroxyl radicals in photocatalysis under visible light [105].

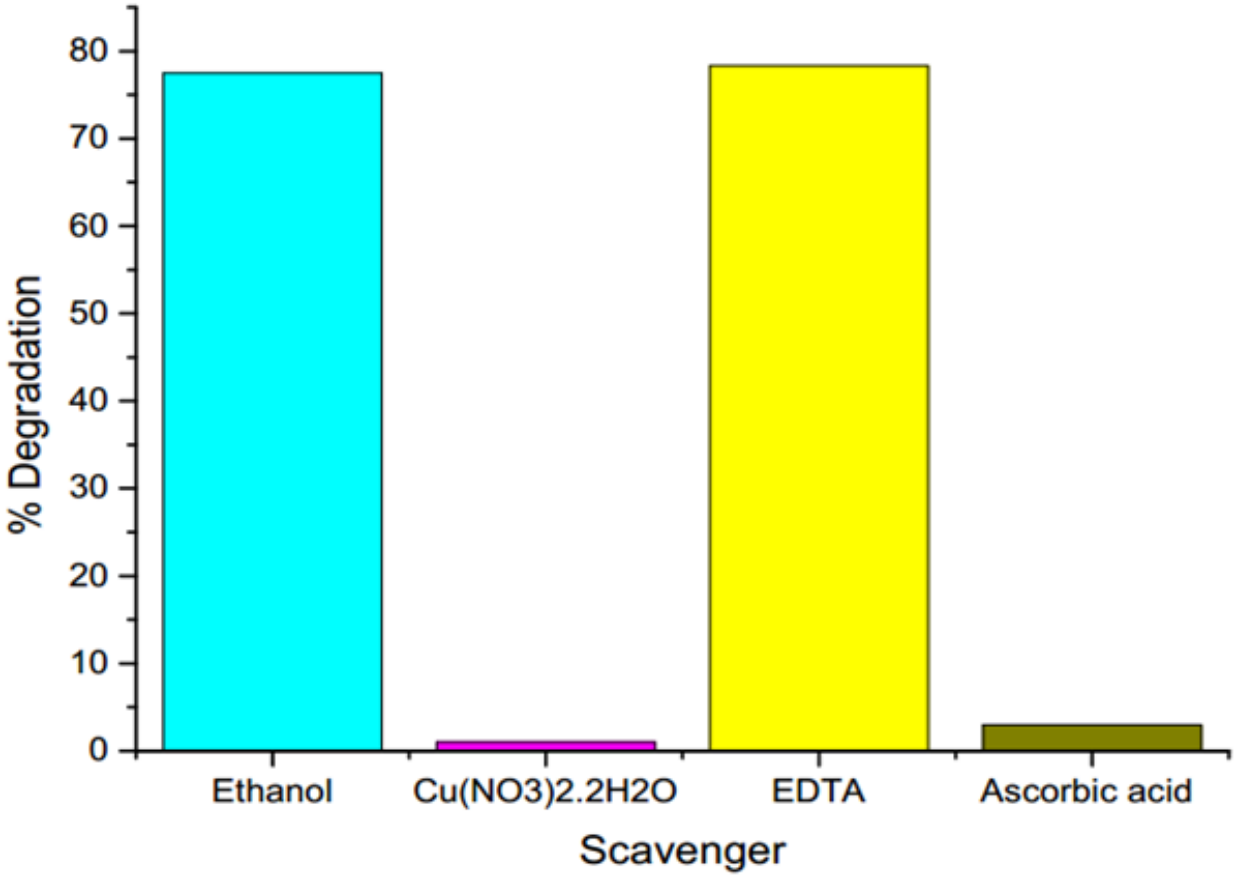

Fig 4.11 Investigation of the mechanism of photocatalytic degradation of MO

As shown in the bar graph above, (Fig 4.10) no significant degradation change took place on the addition of ethanol. This absence of inhibition in the presence of ethanol suggest that the $OH^{\bullet}$ plays a minor role in the photocatalysis of MO. Ascorbic acid was used to probe the formation

and role of $O_2^{\bullet}$. A significant inhibition was observed in the presence of the ascorbic acid as illustrated in Fig 4.7. Yu et al [55] stated that ascorbic acid catalyzes the conversion of $O_2^{\bullet}$ to H_2O_2 and oxygen. Complete inhibition was observed and the degradation of MO was inhibited completely. The superoxide radical anion is a strong oxidizing agent with an electrochemical reduction potential of + 0.89V and can act as an oxidizing agent for the degradation of MO dye [94]. In order to determine the involvement of e^- and h^+ in the photocatalytic degradation of MO, scavenging compounds $Cu(NO)_3 \bullet H_2O$ and EDTA respectively. The Cu^{2+} adsorption onto the surfaces of the ZTC composite decreased the reduction of oxygen by conduction electrons and partially inhibited the formation of reactive oxygen species (ROS) and degradation of MO [64]. The formation of ROS was blocked and this indicated that adsorbed ions can alter the electron transfer pathway thereby suppressing the degradation of MO dye as mentioned by Ajmal et al [106]. The addition of EDTA did not show any significant inhibition in the degradation as shown in Fig 4.10. It can be concluded that the photocatalytic degradation of MO with ZTC composite is influenced by the $O_2^{\bullet}$ radical and the overall mechanism was indirect. This is supported by Pingmuang et al [24] who suggested that if the e^- and the h^+ are not directly reacting with the dye, hence the mechanism is indirect. Significant inhibition of photocatalysis is therefore seen on addition of the ascorbic acid scavenger.

4.12 Recovery and reusability studies of the composite

The ZTC composite photocatalyst was recycled by using the same catalyst portion 5 times. After the optimum conditions for the degradation of MO were determined, the catalyst was recovered by placing a magnet at the bottom of the beaker and the composite beads were attracted to the magnet then the solution was decanted. The beads were washed with distilled water 3 times and again used to study the recyclability.

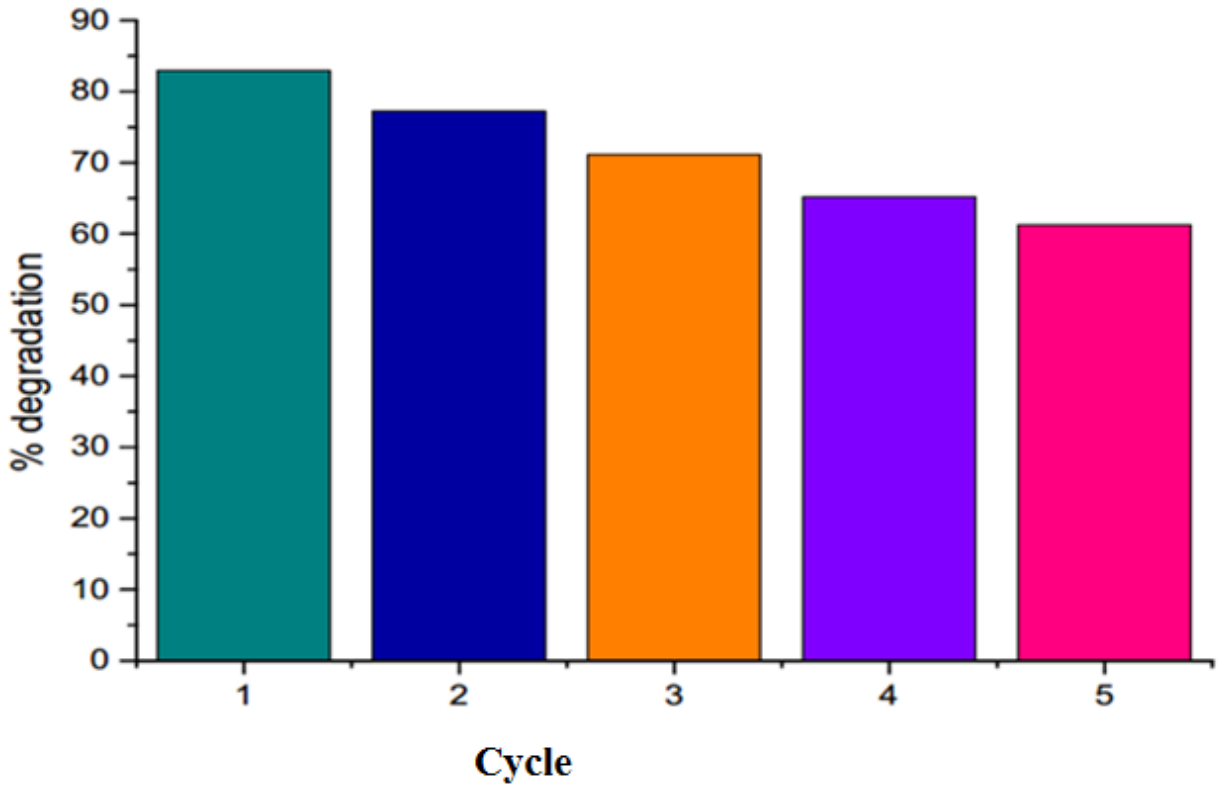

Figure 4.12 Recovery and reusability studies of the composite

The catalyst was recycled four times as shown in Fig 4.11 above. The obtained results showed that the efficiency of the composite decreased from 83 to 61%.

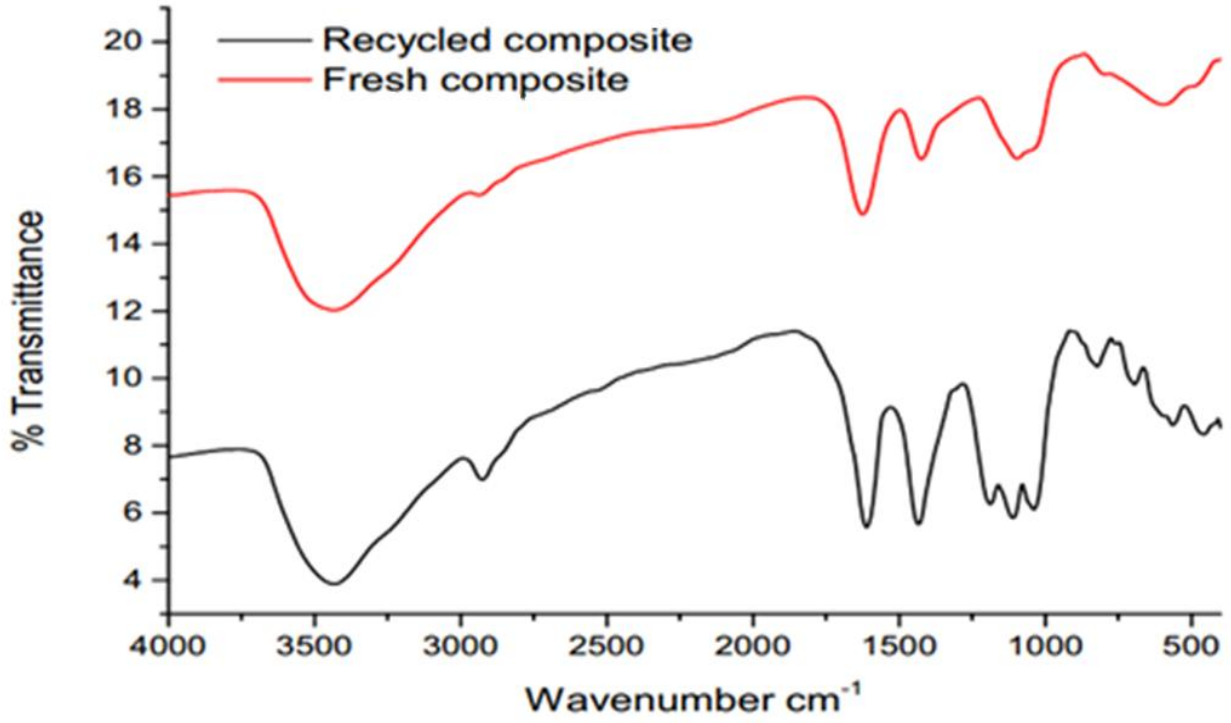

Figure 4.13 FTIR Spectra of the fresh and recycled composite

According to the FTIR of the recycled composite in Fig 4.12, display a peak at 2926 cm^{-1} for asymmetric $–CH_3$ stretching vibrations, peaks at 1611 cm^{-1} represents the C-H bending of aromatic rings. Peaks at 1039 and 695 cm^{-1} for C-H stretching vibrations of the benzene ring and a peak at 822 cm^{-1} for the C-H stretching vibrations in di-substituted benzene ring this confirms aromatic nature of dye. Peak at 1433 cm^{-1} for -N=N-stretching vibrations and peak at 1188 cm^{-1} represents the C-N stretching which also confirm the azo nature of dye. The peak at 1110 cm^{-1} corresponding to the S=O stretching vibrations which confirm the sulfonic nature of the MO.

This may have been the reason for the decrease in the degradation of the MO. These functional groups of MO are as a result of adsorption of the dye on the composite surface thereby masking off some of the surface. This results in less surfaces being available for the release of electrons required for the generation of the active species. Hence, photocatalytic action of the composite

decreased. However, despite the decrease in the degradation of MO, ZTC composite can be used over and over again giving significant dye degradation.

4.13 Stability studies

Stability evaluation of the composite was done by recovering the recycled composite using a piece of magnet. The composite was rinsed rigorously with distilled water three times and dried at 60 ^{0}C for 24 hours. This recovered composite, a sample of fresh composite and alginate beads were digested and analyzed using the AA spectrophotometer. The results shown in Fig 4.12 below were obtained.

Sample	Zn elemental concentration mg	ZnO Concentration: %	Fe elemental concentration mg	$CoFe_2O_4$ Concentration (%)
Fresh composite	7.525	1.8732	15.675	6.585
Recycled composite	7.45	1.8545	15.90	6.6795
Alginate beads	<0.001		<0.001	

Table 4.1 Stability studies of the ZTC composite

It is indicated that the amounts of elements that were obtained shows extensive composite stability. The fresh composite sample had an average of 7.5 mg of the Zn element and 15.7 mg of the Fe element. This represents the ratio of Zn: Fe in the nanoparticles encapsulated in the composite. This ration was also obtained in the recycled sample. This illustrates that the

composite was resistant to metal leaching. Analysis was also done on the amount of Zn present in all the three samples. The amount of zinc reported in the fresh composite and the recycled composite was also found to be almost in the same ratio as the nanoparticles were added into the composite. Zinc was recorded to have an average of 7.45 mg in the recycled composite [107]. The alginate beads were used as a blank sample for the analysis. It exhibited less than 0.001% on all elements. An in-house control sample with a known concentration of the Co, Fe and Zn was used to control the results. All the values obtained were within the accepted range. This validates the methodology used and results obtained. These results were an indication that the fabricated composite was very stable.

CHAPTER 5

CONCLUSION AND RECOMMENDATIONS

5.1 Conclusions

Fabrication of the nano-composite $ZnO/TiO_2/CoFe_2O_4$ was a success and this was applied for the degradation of MO dye. The FTIR characterization confirmed the synthesis due to the vibrational frequencies indicating the presence of the O-H, C-H, aliphatic stretching, asymmetric stretching of the carboxylate salt and the C-O vibration on the alginate. It also confirmed the presence to the nanoparticles due to the broad peak showing in the composite IR spectrum. The decolorisation of MO was witnessed and this confirms that the composite was able to degrade the dye. The optimum conditions for the degradation of MO was found to be pH 8, a contact time of 250 minutes and a catalyst dosage of 0.2 g in 20 mL. The nano-composite was proven to show stability as indicated by the elemental analysis of the composite and the recycled composite which showed no significant change in the amount of the elements after it was used in 5 cycles.

5.2 Recommendations

Application of this developed nano-composite catalyst towards the degradation of other similar organic dyes and pollutants is greatly needed. There is also the need of modifying the alginate beads into carbon spheres without using thermal treatment. The use of ammonium carbonate during the fabrication of beads which then escapes from the alginate solution creating pores necessary for increased surface area for the light to strike through.

REFERENCE LIST

[1] M. Hassaan, A. El Nemr, and M. A. Hassaan, "Health and Environmental Impacts of Dyes: Mini Review," *Am. J. Environ. Sci. Eng.*, vol. 1, no. 3, pp. 64–67, 2017.

[2] S. Rajendran, M. M. Khan, F. Gracia, J. Qin, V. K. Gupta, and S. Arumainathan, "Ce^{3+}-ion-induced visible-light photocatalytic degradation and electrochemical activity of ZnO/CeO_2 nanocomposite," *Sci. Rep.*, vol. 6, pp. 1–11, 2016.

[3] D. Channei, B. Inceesungvorn, N. Wetchakun, S. Ukritnukun, A. Nattestad, J. Chen, and S. Phanichphant, "Photocatalytic degradation of methyl orange by CeO_2 and Fe-doped CeO_2 films under visible light irradiation," *Sci. Rep.*, vol. 4, pp. 1–7, 2014.

[4] R. Article, "Chitosan/Bentonite Nanocomposites for Wastewater Treatment : A Review," *J. Nanochemistry Nanotechnol.*, vol. 1, pp. 1–17, 2018.

[5] J. Kaur, S. Bansal, and S. Singhal, "Photocatalytic degradation of Methyl Orange using ZnO nanopowders synthesized via thermal decomposition of oxalate precursor method," *Phys. B Phys. Condens. Matter*, vol. 13, pp. 1–34, 2013.

[6] P. Peel and M. Strains, "Environmental Treatment of Dyes : Methyl Orange Decolorization Using Hog Plum Peel and Mix-Bacterial Strains," *J. Environ. Sci. Toxicol. Food Technol.*, vol. 5, no. 3, pp. 19–22, 2013.

[7] H. Trabelsi, G. P. Atheba, O. Hentati, Y. D. Mariette, D. Robert, P. Drogui, and M. Ksibi, "Solar photocatalytic decolorization and degradation of methyl orange using supported TiO_2," *J. Adv. Oxid. Technol.*, vol. 19, no. 1, pp. 79–84, 2016.

[8] P. Bhatt and A. Rani, "Textile dyeing and printing industry: An environmental hazard," *Asian Dye.*, vol. 10, no. 6, pp. 51–54, 2013.

[9] J. F. Rumky, Z. Abedin, H. Rahman, and A. Hossain, "Environmental Treatment of Dyes : Methyl Orange Decolorization Using Hog Plum Peel and Mix-Bacterial Strains," *IOSR J. Environ. Sci. Toxicol. Food Technol.*, vol. 5, no. 3, pp. 19–22, 2013.

[10] F. P. Sejie and M. S. Nadiye-tabbiruka, "Removal of Methyl Orange (MO) from Water by adsorption onto Modified Local Clay (Kaolinite)," *J. Phys. Chem.*, vol. 6, no. 2, pp. 39–48, 2016.

[11] L. H. Andrade, A. O. Aguiar, W. L. Pires, G. A. Miranda, L. P. T. Teixeira, G. C. C. Almeida, and M. C. S. Amaral, "Nanofiltration and reverse osmosis applied to gold mining effluent treatment and reuse," *Brazilian J. Chem. Eng.*, vol. 34, no. 1, pp. 93–107, 2017.

[12] A. C. N Vincenzo, "Wastewater Treatment by Combination of Advanced Oxidation Processes and Conventional Biological Systems," *J. Bioremediation Biodegrad.*, vol. 4, no. 8, pp. 200–208, 2013.

[13] S. Al-Qaradawi and S. R. Salman, “Photocatalytic degradation of methyl orange as a model compound,” *J. Photochem. Photobiol. A Chem.*, vol. 148, no. 1, pp. 161–168, 2012.

[14] P. Lu, Y. Jing, Q. Zhang, H. Ying, and L. Li, “Photocatalytic Degradation of Methyl Orange by Chitosan Modified TiO_2,” *Conf. Environ. Pollut. Public Heal. Vol 1-2*, pp. 888–891, 2010.

[15] X. Chen, Z. Wu, D. Liu, and Z. Gao, “Preparation of ZnO Photocatalyst for the Efficient and Rapid Photocatalytic Degradation of Azo Dyes,” pp. 4–13, 2017.

[16] Y.-S. Wong, M. Rafatullah, S.-A. Ong, Y.-Y. Lau, T.-T. Teng, and N. Morad, “Degradation of cationic and anionic dyes in coagulation–flocculation process using bi-functionalized silica hybrid with aluminum-ferric as auxiliary agent,” *RSC Adv.*, vol. 5, no. 43, pp. 34206–34215, 2015.

[17] G. Ucankus, M. Ercan, D. Uzunoglu, and M. Culha, *Methods for preparation of nanocomposites in environmental remediation*. Elsevier Inc., 2018.

[18] P. Pal, “Treatment and Disposal of Pharmaceutical Wastewater: Toward the Sustainable Strategy,” *Sep. Purif. Rev.*, vol. 47, no. 3, pp. 179–198, 2018.

[19] R. Gong, J. Ye, W. Dai, X. Yan, J. Hu, X. Hu, S. Li, and H. Huang, “Adsorptive removal of methyl orange and methylene blue from aqueous solution with finger-citron-residue-based activated carbon,” *Ind. Eng. Chem. Res.*, vol. 52, no. 39, pp. 14297–14303, 2013.

[20] M. S. Nawaz and M. Ahsan, “Comparison of physico-chemical, advanced oxidation and biological techniques for the textile wastewater treatment,” *Alexandria Eng. J.*, vol. 53, no. 3, pp. 717–722, 2014.

[21] V. N. Nguyen, D. T. Tran, M. T. Nguyen, T. T. T. Le, M. N. Ha, M. V. Nguyen, and T. D. Pham, “Enhanced photocatalytic degradation of methyl orange using ZnO/graphene oxide nanocomposites,” *Res. Chem. Intermed.*, vol. 44, no. 5, pp. 3081–3095, 2018.

[22] X. Chen, Z. Wu, D. Liu, and Z. Gao, “Preparation of ZnO Photocatalyst for the Efficient and Rapid Photocatalytic Degradation of Azo Dyes,” *Nanoscale Res. Lett.*, vol. 12, no. 1, pp. 4–13, 2017.

[23] R. Saravanan, N. Karthikeyan, S. Govindan, V. Narayanan, and A. Stephen, “Photocatalytic Degradation of Organic Dyes Using Nanocomposite material under Visible Light,” *Adv. Mater. Res.*, vol. 584, pp. 381–385, 2012.

[24] K. Pingmuang, J. Chen, W. Kangwansupamonkon, G. G. Wallace, S. Phanichphant, and A. Nattestad, “Composite Photocatalysts Containing $BiVO_4$ for Degradation of Cationic Dyes,” *Sci. Rep.*, vol. 7, no. 1, 2017.

[25] S. R. Bammidi, “Synthesis and Characterizati of Zinc Oxide Nanoparticles and its Antimicrobial Activity against Bacillus Subtilis and Escherichia Coli,” *Rasayan J. Chem.*, vol. 4, no. 1, pp. 217–222, 2011.

[26] X. Shang, B. Li, T. Zhang, C. Li, and X. Wang, “Photocatalytic Degradation of Methyl Orange with Commercial Organic Pigment Sensitized TiO_2,” *Procedia Environ. Sci.*, vol. 18, pp. 478–485, 2013.

[27] R. Saravanan, F. Gracia, and A. Stephen, “Basic Principles , Mechanism and Challenges of Photocatalysis,” *Polym. Compos. Mater.*, vol. 2, pp. 19–41, 2017.

[28] T. Chen, Y. Zheng, J. M. Lin, and G. Chen, “Study on the Photocatalytic Degradation of Methyl Orange in Water Using Ag/ZnO as Catalyst by Liquid Chromatography Electrospray Ionization Ion-Trap Mass Spectrometry,” *J. Am. Soc. Mass Spectrom.*, vol. 19, no. 7, pp. 997–1003, 2008.

[29] Y. O. López, H. M. Vázquez, J. S. Gutiérrez, V. G. Velderrain, A. L. Ortiz, and V. C. Martínez, “Synthesis Method Effect of $CoFe_2O_4$ on Its Photocatalytic Properties for H2 Production from Water and Visible Light,” *J. Nanotechnol.*, vol. 15, pp. 1–9, 2015.

[30] Y. Konishi, T. Nomura, K. Mizoe, and K. Nakata, “Preparation of Cobalt Ferrite Nanoparticles by Hydrolysis of Cobalt-Iron (III) Carboxylate Dissolved in Organic Solvent,” *Mater. Trans.*, vol. 45, no. 1, pp. 81–85, 2014.

[31] J. Ebenezar, C. Growth, and Q. Dots, “Synthesis and characterization of Cobalt Ferrite Nanoparticles Prepared by Hydrothermal Method,” *Recent Trends Mater. Sci. Appl.*, vol. 189, pp. 146–152, 2017.

[32] S. Huang, Y. Xu, M. Xie, H. Xu, M. He, J. Xia, L. Huang, and H. Li, "Synthesis of magnetic $CoFe_2O_4$/g-C_3N_4 composite and its enhancement of photocatalytic ability under visible-light," *Colloids Surfaces A Physicochem. Eng. Asp.*, vol. 478, pp. 71–80, 2015.

[33] M. Lee, B.-Y. Chen, and W. Den, "Chitosan as a Natural Polymer for Heterogeneous Catalysts Support: A Short Review on Its Applications," *Appl. Sci.*, vol. 5, no. 4, pp. 1272–1283, 2015.

[34] D. Kanakaraju, S. Ravichandar, and Y. C. Lim, "Combined effects of adsorption and photocatalysis by hybrid TiO_2/ZnO-calcium alginate beads for the removal of copper," *J. Environ. Sci. (China)*, vol. 55, pp. 214–223, 2017.

[35] Y. Dong, W. Dong, Y. Cao, Z. Han, and Z. Ding, "Preparation and catalytic activity of Fe alginate gel beads for oxidative degradation of azo dyes under visible light irradiation," *Catal. Today*, vol. 175, no. 1, pp. 346–355, 2011.

[36] Y. Li, K. Sui, R. Liu, X. Zhao, Y. Zhang, H. Liang, and Y. Xia, "Energy Procedia Removal of Methyl Orange from Aqueous Solution by Calcium Alginate / Multi-walled Carbon Nanotubes Composite Fibers," *Energy Procedia*, vol. 16, pp. 863–868, 2012.

[37] K. Huang, A. M. Grumezescu, C. Chang, C. Yang, and C. Wang, "Immobilization and Stabilization of TiO_2 Nanoparticles in Alkaline- Solidifiecated Chitosan Spheres without crosslinking agent," *Int. J. Latest Res. Sci. Technol.*, vol. 3, no. 2, pp. 174–178, 2014.

[38] L. Zhao, L. Shi, Z. Zhang, J. Chen, D. Shi, J. Yang, and Z. Tang, "Preparation And Application Of Chitosan Nanoparticles And Nanofibers," *Brazilian J. Chem. Eng.*, vol. 28, no. 03, pp. 353–362, 2011.

[39] H. Jonassen, A. Kjøniksen, and M. Hiorth, "Stability of Chitosan Nanoparticles Cross-Linked with Tripolyphosphate," *Biomacromolecules*, vol. 13, pp. 3747–3756, 2012.

[40] E. Alzahrani, "Chitosan Membrane Embedded With ZnO / CuO Nanocomposites for the Photodegradation of Fast Green Dye Under Artificial and Solar Irradiation," *Int. J. Carbohydr. Chem.*, vol. 12, pp. 1–6, 2018.

[41] F. Science, "Preparation of chitosan beads using Tripolyphosphate Ethylene Glycol Diglycidyl Ether as crosslinker for Cr (VI) adsorption," *J. Chem. Chem. Technol.*, vol. 10, no. 1, pp. 105–114, 2016.

[42] X. Luo, X. Lei, N. Cai, X. Xie, Y. Xue, and F. Yu, "Removal of heavy metal ions from water by magnetic cellulose-based beads with embedded chemically modified magnetite nanoparticles and activated carbon," *ACS Sustain. Chem. Eng.*, vol. 4, no. 7, pp. 3960–3969, 2016.

[43] R. Sasikala, K. Karthikeyan, D. Easwaramoorthy, I. M. Bilal, and S. K. Rani, "Photocatalytic degradation of trypan blue and methyl orange azo dyes by cerium loaded CuO nanoparticles," *Environ. Nanotechnology, Monit. Manag.*, vol. 6, pp. 45–53, 2016.

[44] M. I. H. Chowdhury, M. S. Hossain, M. A. S. Azad, M. Z. Islam, and M. A. Dewan, "Photocatalytic Degradation of Methyl Orange Under UV Using ZnO as Catalyst," *Int. J. Sci. Eng. Res.*, vol. 9, no. 6, 2018.

[45] P. Sivakumar and P. N. Palanisamy, "Low-cost non-conventional activated carbon for the removal of Reactive Red 4: Kinetic and isotherm studies," *Rasayan J. Chem.*, vol. 1, no. 4, pp. 871–883, 2008.

[46] K. Milenova, K. Milenova, K. Zaharieva, I. Stambolova, V. Blaskov, A. Eliyas, and L. Dimitrov, "Photocatalytic performance of TiO_2, CeO_2, ZnO and TiO_2-CeO_2-ZnO in the course of Methyl Orange dye degradation," *J. Chem. Technol. Metall.*, vol. 52, no. 1, pp. 13–19, 2017.

[47] M. Pirilä, M. Saouabe, S. Ojala, B. Rathnayake, F. Drault, A. Valtanen, M. Huuhtanen, R. Brahmi, and R. L. Keiski, "Photocatalytic Degradation of Organic Pollutants in Wastewater," *Top. Catal.*, vol. 58, no. 14–17, pp. 1085–1099, 2015.

[48] N. Kislov, J. Lahiri, H. Verma, D. Y. Goswami, E. Stefanakos, and M. Batzill, "Photocatalytic degradation of methyl orange over single crystalline ZnO: Orientation dependence of photoactivity and photostability of ZnO," *Am. Chem. Soc.*, vol. 25, no. 5, pp. 3310–3315, 2009.

[49] I. Fajriati, Mudasir, and E. T. Wahyuni, "Photocatalytic decolorization study of methyl orange by TiO_2-chitosan nanocomposites," *Indones. J. Chem.*, vol. 14, no. 3, pp. 209–218,

2014.

[50] M. Ge, C. Guo, X. Zhu, L. Ma, Z. Han, W. Hu, and Y. Wang, “Photocatalytic degradation of methyl orange using ZnO/TiO_2 composites,” *Front. Environ. Sci. Eng. China*, vol. 3, no. 3, pp. 271–280, 2009.

[51] Q. Feng, S. Li, W. Ma, H. J. Fan, X. Wan, Y. Lei, Z. Chen, J. Yang, and B. Qin, “Synthesis and characterization of Fe_3O_4/ZnO-GO nanocomposites with improved photocatalytic degradation methyl orange under visible light irradiation,” *J. Alloys Compd.*, vol. 737, pp. 197–206, 2018.

[52] T. Montini, M. Melchionna, M. Monai, and P. Fornasiero, “Fundamentals and Catalytic Applications of CeO_2-Based Materials,” *Chem. Rev.*, vol. 116, no. 10, pp. 5987–6041, 2016.

[53] E. Bazrafshan, A. A. Zarei, H. Nadi, and M. A. Zazouli, “Adsorptive removal of Methyl Orange and Reactive Red 198 dyes by Moringa peregrina ash,” *Indian J. Chem. Technol.*, vol. 21, pp. 105–113, 2014.

[54] A. I. Molla, M. Furukawa, I. Tateishi, and H. Katsumata, “Photocatalytic Decolorization of Dye with Self-Dye-Sensitization under Fluorescent Light Irradiation,” *Chem. Eng. J.*, vol. 1, no. 8, pp. 1–10, 2017.

[55] L. Yu, S. Polytech, J. Xi, H. T. Chan, D. C. Company, and D. L. Phillips, “The

Degradation Mechanism of Methyl Orange Under Photo-Catalysis of TiO_2," *Phys. Chem. Chem. Phys.*, vol. 14, pp. 3589–3595, 2012.

[56] N. Guettaï and H. Ait Amar, "Photocatalytic oxidation of methyl orange in presence of titanium dioxide in aqueous suspension. Part I: Parametric study," *Desalination*, vol. 185, pp. 427–437, 2005.

[57] M. T. Yagub, T. K. Sen, S. Afroze, and H. M. Ang, "Dye and its removal from aqueous solution by adsorption: A review," *Adv. Colloid Interface Sci.*, vol. 209, pp. 172–184, 2014.

[58] F. I. Hai, K. Yamamoto, and K. Fukushi, "Hybrid treatment systems for dye wastewater," *Crit. Rev. Environ. Sci. Technol.*, vol. 37, no. 4, pp. 315–377, 2007.

[59] B. T. Huy, C. Thi, B. Thao, V. Dao, N. Thi, K. Phuong, and Y. Lee, "A Mixed-Metal Oxides / Graphitic Carbon Nitride : High Visible Light Photocatalytic Activity for Efficient Mineralization of Rhodamine B," *Adv. Mater. Interfaces*, pp. 1–9, 2017.

[60] G. Boczkaj and A. Fernandes, "Wastewater treatment by means of advanced oxidation processes at basic pH conditions : A review," *Chem. Eng. J.*, vol. 320, pp. 608–633, 2017.

[61] W. Szeto, C. W. Kan, C. W. M. Yuen, S. Chan, and K. H. Lam, "Effective Photodegradation of Methyl Orange Using Fluidized Bed Reactor Loaded with Cross-Linked Chitosan Embedded Nano-CdS Photocatalyst," *Int. J. Chem. Eng.*, pp. 18–20,

2014.

[62] Y. Iida, T. Kozuka, T. Tuziuti, and K. Yasui, “Sonochemically enhanced adsorption and degradation of methyl orange with activated aluminas,” *Ultrasonics*, vol. 42, pp. 635–639, 2014.

[63] A. S. Stasinakis, “Use of selected advanced oxidation processes for waste water treatment,” *Glob. NEST J.*, vol. 10, no. 3, pp. 376–385, 2016.

[64] N. and A. Y. Yoshio, “Fundamentals : Active Species , Mechanisms , Reaction Pathways,” *Photocatal. Water Purif.*, vol. 13, pp. 1–24, 2013.

[65] D. Mishra, K. K. Senapati, C. Borgohain, and A. Perumal, “$CoFe_2O_4$ – Fe_3O_4 Magnetic Nanocomposites as Photocatalyst for the Degradation of Methyl Orange Dye,” *J. Nanotechnol.*, vol. 12, pp. 1–12, 2012.

[66] C. Hariharan, “Photocatalytic degradation of organic contaminants in water by ZnO nanoparticles: Revisited,” *Appl. Catal. A Gen.*, vol. 304, no. 1–2, pp. 55–61, 2006.

[67] E. Alzahrani, “Chitosan Membrane Embedded With ZnO / CuO Nanocomposites for the Photodegradation of Fast Green Dye Under Artificial and Solar Irradiation,” *Anal. Chem. Insights*, vol. 13, pp. 1–13, 2018.

[68] W. Li, D. Li, Y. Lin, P. Wang, W. Chen, X. Fu, and Y. Shao, “Evidence for the Active

Species Involved in the Photodegradation Process of Methyl Orange on TiO_2," *J. Phys. Chem.*, vol. 2, no. 116, pp. 3552–3560, 2012.

[69] R. Saravanan, H. Shankar, G. Rajasudha, A. Stephen, G. Campus, V. Narayanan, and G. Campus, "Photocatalytic Degradation of Organic Dye using Nano ZnO," *Int. J. Nanosci.*, vol. 10, no. 1, pp. 253–257, 2011.

[70] S. Prabhu, T. Viswanathan, K. Jothivenkatachalam, and K. Jeganathan, "Visible Light Photocatalytic Activity of CeO_2-ZnO-TiO_2 Composites for the Degradation of Rhodamine B," *Indian J. Mater. Sci.*, vol. 14, pp. 1–10, 2014.

[71] S. Jurablu, M. Farahmandjou, and T. P. Firoozabadi, "Sol-Gel Synthesis of Zinc Oxide (ZnO) Nanoparticles : Study of Structural and Optical Properties," *J. Sci.*, vol. 26, no. 3, pp. 281–285, 2015.

[72] J. N. Hasnidawani, H. N. Azlina, H. Norita, N. N. Bonnia, S. Ratim, and E. S. Ali, "Synthesis of ZnO Nanostructures Using Sol-Gel Method Synthesis of ZnO Nanostructures Using Sol-Gel Method," *Procedia Chem.*, vol. 19, pp. 211–216, 2016.

[73] R. Ullah and J. Dutta, "Photocatalytic degradation of organic dyes with manganese-doped ZnO nanoparticles," *J. Hazard. Mater.*, vol. 156, no. 1–3, pp. 194–200, 2008.

[74] S. D. Kulkarni, S. Kumbar, S. G. Menon, K. S. Choudhari, and C. Santhosh, "Magnetically separable core-shell $ZnFe_2O_4$/ZnO nanoparticles for visible light

photodegradation of methyl orange," *Mater. Res. Bull.*, vol. 77, pp. 70–77, 2016.

[75] V. N. Nguyen, D. Trinh, T. Manh, and T. Nguyen, "Enhanced photocatalytic degradation of methyl orange using ZnO / graphene oxide nanocomposites," *Res. Chem. Intermed.*, vol. 8, no. 17, 2018.

[76] M. F. Romadhan, N. E. Suyatma, and F. M. Taqi, "Synthesis of ZnO Nanoparticles by Precipitation Method with Their Antibacterial Effect," *Indones. J. Chem.*, vol. 16, no. 2, pp. 117–123, 2016.

[77] K. and G. P. Azad, "Photodegradation of Methyl Orange in Aqueous Solution by the Visible Light Active Co : La : TiO_2 Nanocomposite," *Chem. Sci. J.*, vol. 8, no. 3, 2017.

[78] N. Barka and A. Assabbane, "Photocatalytic degradation of methyl orange with immobilized TiO_2 nanoparticles : effect of pH and some inorganic anions," *Phys. Chem. News*, vol. 41, pp. 85–88, 2008.

[79] T. Tatarchuk, M. Bououdina, J. J. Vijaya, and L. J. Kennedy, "Spinel Ferrite Nanoparticles : Synthesis , Crystal Structure , Properties , and Perspective Applications," *Nanophysics, Nanomater. Interface staudies Appl.*, vol. 195, pp. 305–325, 2017.

[80] Y. O. Lopez, H. M. Vazquez, J. S. Gutierrez, V. G. Velderrain, A. L. Ortiz, and V. C. Martinez, "Synthesis method effect of $CoFe_2O_4$ on its photocatalytic properties for H_2 production from water and visible light.," *J. Nanomater.*, vol. 3, pp. 1–12, 2014.

[81] L. Sun and F. Bunshi, “Effect of encapsulated graphene oxide on alginate-based bead adsorption to remove acridine orange from aqueous solutions,” pp. 1–22, 2016.

[82] A. Lewandowska and K. Winnicka, “The Influence of Chitosan Cross-linking on the Properties of Alginate Microparticles with Metformin Hydrochloride — In Vitro and In Vivo Evaluation,” *Molecules*, vol. 22, no. 182, pp. 1–20, 2017.

[83] F. Ismail and A. El, “Synthesis and Study of Superparamagnetic (Fe_3O_4/ (Chitosan / alginate) - co-acrylic acid) Nanocomposite for Different Applications,” *Int. J. Nanomater. Chem.*, vol. 10, no. 1, pp. 5–10, 2016.

[84] H. Koohestani and S. K. Sadrnezhaad, “Photocatalytic degradation of methyl orange and cyanide by using TiO_2 / CuO composite,” *Desalin. Water Treat.*, vol. 14, no. 32, 2016.

[85] W. Szeto, C. W. Kan, C. W. M. Yuen, S. W. Chan, and K. H. Lam, “Effective Photodegradation of Methyl Orange Using Fluidized Bed Reactor Loaded with Cross-Linked Chitosan Embedded Nano-CdS Photocatalyst,” *Int. J. Chem. Eng.*, vol. 2014, pp. 18–20, 2014.

[86] S. S. Alias, A. B. Ismail, and A. A. Mohamad, “Effect of pH on ZnO nanoparticle properties synthesized by sol – gel centrifugation,” *J. Alloys Compd.*, vol. 499, no. 2, pp. 231–237, 2012.

[87] D. Davis and S. Singh, “ZnO Nanoparticles Synthesis by Sol-gel Method and

Characterization," vol. 4, no. 1, pp. 4–7, 2016.

[88] Y. Xu, C. Zhan, L. Fan, L. Wang, and H. Zheng, "Preparation of dual crosslinked alginate-chitosan blend gel beads and in vitro controlled release in oral site-specific drug delivery system," *Int. J. Pharm.*, vol. 336, no. 2, pp. 329–337, 2007.

[89] C. Zhao, Q. Yan, S. Wang, P. Dong, and L. Zhang, "Regenerable g-C_3N_4 –chitosan beads with enhanced photocatalytic activity and stability," *RSC Adv.*, vol. 8, no. 48, pp. 27516–27524, 2018.

[90] C. E. Corcione and M. Frigione, "Characterization of Nanocomposites by Thermal Analysis," pp. 2960–2980, 2012.

[91] M. Joshi, A. Bhattacharyya, and S. W. Ali, "Characterization techniques for nanotechnology applications in textiles," *J. Nanotechnol.*, vol. 33, no. September, pp. 304–317, 2008.

[92] R. Dermy, R. C, Sinclaire, "Validating UV / Visible Spectrophotometers," in *Visible Ultraviolet Spectroscopy*, 2012.

[93] A. K and G. P, "Photodegradation of Methyl Orange in Aqueous Solution by the Visible Light Active Co:La:TiO2 Nanocomposite," *Chem. Sci. J.*, vol. 08, no. 03, pp. 164–172, 2017.

[94] A. I. Molla, I. Tateishi, M. Furukawa, H. Katsumata, and T. Suzuki, “Evaluation of Reaction Mechanism for Photocatalytic Degradation of Dye with Self-Sensitized TiO_2 under Visible Light Irradiation,” *Open J. Inorg. Non-Metallic Mater.*, vol. 7, no. 1, pp. 1–7, 2017.

[95] G. Hou, Y. Li, W. An, S. Gao, W. Zhang, and W. Cui, “Fabrication and photocatalytic activity of magnetic core shell $ZnFe_2O_4/Ag_3PO_4$ heterojunction,” *Mater. Sci. Semicond. Process.*, vol. 63, pp. 261–268, 2017.

[96] D. Effects, F. M. Omar, H. A. Aziz, and S. Stoll, “Stability of ZnO Nanoparticles in Solution . Influence of pH , Dissolution , Aggregation Stability of ZnO Nanoparticles in Solution . Influence of pH , Dissolution , Aggregation and Disaggregation Effects,” *J. Colloid Sci. Biotechnol.*, vol. 3, pp. 1–10, 2014.

[97] J. N. Hasnidawani, H. N. Azlina, H. Norita, and N. N. Bonnia, “Synthesis of ZnO Nanostructures Using Sol-Gel Method,” *Procedia Chem.*, vol. 19, pp. 211–216, 2016.

[98] Z. Liu, R. Wang, F. Kan, and F. Jiang, “Synthesis and characterization of TiO_2 Nanoparticles,” *Asian J. Chem.*, vol. 26, no. 3, pp. 655–659, 2014.

[99] J. Prakash, A. Tripathi, J. C. Pivin, J. Tripathi, A. K. Chawla, and R. Chandra, “Study on synthesis of magnetic nanocomposite (Ni-Teflon) by swift heavy ion beam mixing,” *Adv. Mater. Lett.*, vol. 2, no. 1, pp. 71–75, 2011.

[100] N. A. Salahuddin, M. El-kemary, and E. M. Ibrahim, “Synthesis and Characterization of ZnO Nanoparticles via Precipitation Method : Effect of Annealing Temperature on Particle Size,” *J. Nanosci. Nanotechnol.*, vol. 5, no. 4, pp. 82–88, 2015.

[101] P. M. Aneesh, K. A. Vanaja, and M. K. Jayaraj, “Synthesis of ZnO nanoparticles by hydrothermal method,” *Nanophotonic Mater. IV*, vol. 6639, no. 2007, 2007.

[102] F. B. D. and H. C. S. L F Koao, “Effect of pH on the properties of ZnO nanostructures prepared by chemical bath deposition method,” *SA Inst. Phys.*, pp. 43–48, 2015.

[103] N. Barka and A. Assabbane, “Photocatalytic degradation of methyl orange with immobilized TiO_2 nanoparticles : effect of pH and some inorganic anions,” *Phys. Chem. News*, vol. 41, pp. 85–88, 2008.

[104] V. Augugliaro, V. Loddo, G. Marcì, L. Palmisano, and M. J. López-Muñoz, “Photocatalytic oxidation of cyanides in aqueous titanium dioxide suspensions,” *J. Catal.*, vol. 166, no. 2, pp. 272–283, 1997.

[105] R. Saravanan, F. Gracia, and A. Stephen, “Basic Principles , Mechanism , and Challenges of Photocatalysis,” *Polym. Compos. Mater.*, vol. 4, pp. 19–41, 2017.

[106] A. Ajmal, I. Majeed, and N. Malik, “Principles and mechanisms of photocatalytic dye degradation on TiO_2 based photocatalysts : a,” *R. Soc. Chem.*, vol. 4, pp. 37003–37026, 2014.

[107] W. Srithammavut, S. Luukkanen, A. Laari, T. Kankaanpää, and I. Turunen, "Kinetic Modelling of Gold Leaching and Cyanide Consumption in Intensive Cyanidation of Refractory Gold Concentrate," *J. Univ. Chem. Technol. Metall.*, vol. 46, no. 2, pp. 181–190, 2011.

APPENDIX

APPENDIX A: MATERIALS

List A1: apparatus used for the study

Beakers, Volumetric Flasks, spatula, sample vials, centrifuge tubes, funnels, weighing crucibles, Erlenmeyer Flask, water bath, hot plate, magnetic stirrer, measuring cylinder, burette, syringes, cuvettes, stop watch, and cuvettes.

Table A1: reagents

Chemical Name	Chemical formula	Manufacturer	Concentration/ mass
Distilled water	H_2O	MSU Lab	_
Hydrochloric acid	HCl	Glassworld	0.1 M
Ascorbic acid	$C_6H_8O_6$	ACE	1g
Ferric Nitrate	Fe $(NO_3)_3.9H_2O$	ACE	8g
Cobalt Nitrate	Co $(NO_3)_{2.}6H_2O$	Skylab	4g
Titanium dioxide	TiO_2	_	5g

Methyl orange dye	$C_{14}H_{14}N_3NaO_3S$	Skylab's	50 g
Zinc acetate	$Zn(CH_3CO_2)_2$	-	20g
Sodium hydroxide	NaOH	Skylab's	10M
Ethanol	CH_3CH_2OH	Glassworld	99%
Cupric Nitrate	$Cu(NO_3)_2.2H_2O$	ACE	0.5g
Sodium alginate	$C_6H_9NaO_7$	_	5g
Sodium Chloride	NaCl	ACE	1g
Disodium edetate	Na_2EDTA	ACE	0.5g

Table A2: Instrumentation

Name	**Model**	**Manufacturer**	**Use**
Analytical Balance	GA-110	OHAUS	Weighing
FAAS	200 Series AA	Agilent Technologies	Elemental analysis
FTIR	Nicolet 6700	Thermo Scientific	Analysis of functional groups
SAED			Analysis of crystal structure

TGA	TGA550	Advanced laboratory Solutions	Thermal stability
TEM			Determination of the size
Ultra-Sonicator	KQ-250B	China Corp	Particle dispersion
pH meter	Az-8601	OHAUS	Obtaining Ph
UV vis spectrophotometer	2000 series	Digilab Merlin USA	MO quantification
Oven	DHG-9070	Melrose	Drying
Muffle furnace	MFAT302F	Auto Lab	Calcining
Centrifuge	GB004	Cliffton	Particle Isolation

APENDIX B: RAW DATA FOR LABORATORY EXPERIMENTS

Fig B0: Calibration curve used for the quantification of MO

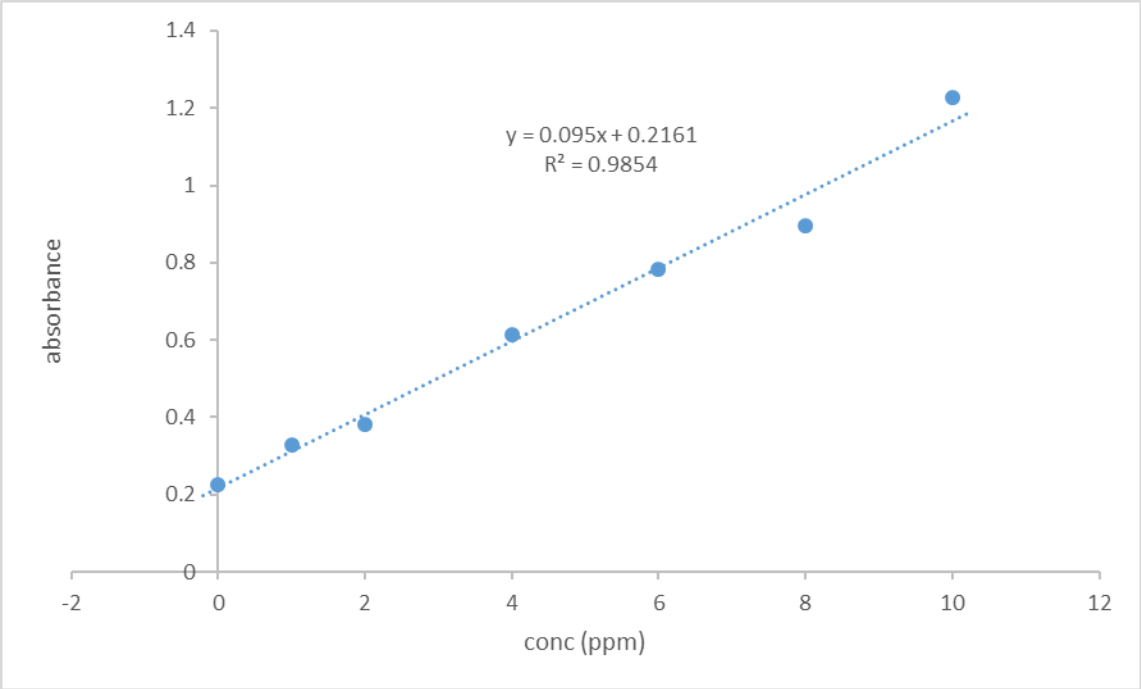

Figure BO Calibration curve used for the quantification of MO

Table B1: Raw data on the effect of pH on the performance of the composite.

pH	absorbance	Run 1	Run 2	Average
6	initial	0.861	0.861	0.861
	final	0.397	0.391	0.394
7	initial	0.858	0.857	0.858

	final	0.326	0.322	0.324
8	initial	0.866	0.869	0.868
	final	0.278	0.286	0.282
9	initial	0.871	0.869	0.870
	final	0.429	0.427	0.428
10	initial	0.886	0.887	0.887
	final	0.711	0.723	0.717
adsorption control	initial	0.861		0.861
	final	0.731		0.731
photodegradation control	initial	0.862		0.862
	final	0.843		0.843

Table B2: Raw data for the effect of concentration on degradation

Concentration/ppm	absorbance	Run 1	Run 2	Average
1	initial	0.330	0.332	0.331
	final	0.645	0.674	0.660
5	initial	0.714	0.718	0.716

	final	0.437	0.476	0.457
10	initial	0.816	0.818	0.817
	final	0.400	0.416	0.408
15	initial	1.226	1.230	1.228
	final	0.426	0.450	0.438
20	initial	1.460	1.467	1.464
	final	0.514	0.545	0.530
25	initial	1.675	1.675	1.675
	final	0.641	0.843	0.742
100	initial	0.967	0.966	0.967
	final	0.068	0.069	0.069
adsorption control	initial	0.817		0.817
	final	0.796		0.796
photodegradation control	initial	0.815		0.815
	final	0.814		0.814

Table B3: Raw data for the effect of time on the degradation

time/min	Column1	Run 1	Run 2	Average
0	initial	0.879	0.865	0.872
30	final	0.803	0.812	0.808
60	final	0.716	0.801	0.759
90	final	0.682	0.711	0.697
120	final	0.503	0.569	0.536
150	final	0.487	0.446	0.467
180	final	0.381	0.369	0.375
210	final	0.372	0.369	0.371
240	final	0.370	0.371	0.371
270	final	0.364	0.362	0.363
300	final	0.360	0.358	0.359
adsorption control	initial	0.882		0.882
	final	0.757		0.757
photodegradation control	initial	0.878		0.878
	final	0.881		0.881

Table B4: Raw data for the effect of catalyst dosage on the degradation

Catalyst dosage/g	Absorbance	Run 1	Run 2	Average
	initial	0.885	0.887	0.886
0.05	final	0.429	0.419	0.424
0.1	final	0.407	0.403	0.405
0.15	final	0.392	0.386	0.389
0.2	final	0.371	0.369	0.37
0.25	final	0.4	0.408	0.404
0.3	final	0.423	0.402	0.4125
0.5	final	0.361	0.358	0.3595
1	final	0.355	0.338	0.3465
adsorption control	final	0.827		0.827
photodegradation control		0.883		0.883

Table B5: Raw data for the photocatalytic degradation of MO under optimum conditions

Sample	Initial absorbance	Final absorbance
Run 1	0.865	0.237
Run 2	0.865	0.264
Run 3	0.863	0.213

Table B6: Raw data for the mechanism investigation

Scavenger	Absorbance	Run 1	Run 2	Average
	initial	0.892	0.896	0.894
Ethanol	final	0.429	0.431	0.43
Cu(NO3)2.2H2O	final	0.559	0.567	0.563
EDTA	final	0.365	0.342	0.3535
Ascorbic acid	final	0.408	0.437	0.4225
adsorption control	final	0.889		0.889
photodegradation control	final	0.893		0.893

Table B7: Raw data for the recovery and reusability studies of the catalyst

Cycle	Absorbance	Run 1	Run 2	Average
1	initial	0.886	0.88	0.883
	final	0.378	0.378	0.378
2	initial	0.875	0.879	0.877
	final	0.401	0.463	0.432
3	initial	0.893	0.892	0.893
	final	0.489	0.491	0.490
4	initial	0.874	0.874	0.874
	final	0.536	0.558	0.547
5	initial	0.881	0.88	0.881
	final	0.576	0.593	0.585

Table B8 Raw data for the stability studies of the composite

Sample	ZnO AA reading	Co AA reading	Fe AA reading
Fresh composite 1	3.02	3.76	6.41
Fresh composite 2	2.99	3.73	6.12
Recycled composite 1	2.90	3.57	6.42
Recycled composite 2	3.07	3.62	6.31
Alginate beads 1	<0.01	<0.01	<0.01
Alginate beads 2	<0.01	<0.01	<0.01
RD1	544	54	576

APENDIX C: DATA TREATMENT STRATEGIES

Several data treatment strategies were used. These included formulas used to come up with several data sets. The first one is the mean/ average and it is shown below:

$$\text{Mean}(\mu) = \frac{\sum x}{n}$$

The photocatalytic degradation efficiency was calculated as follows:

$$\%\ \text{degradation} = \frac{C0 - C1}{C0} * 100$$

Where, C0 and C1 correspond to the initial and final concentration of dye before and after photocatalytic degradation.

CUSTOMER: MARVELOUS MIRASO

RIOZIM LIMITED
CENTRAL ANALYTICAL LABORATORY
EIFFEL FLATS

SOLIDS

BATCH NO.	SAMPLE DATES	RECEIVED DATE	ANALYSIS DATE	SAMPLE DESCRIPTION	Co %	Fe %	Zn %				
20190506113	06.05.2019	06.05.2019	06.05.2019	Comp 1	25	42	20				
"	"	"	"	Comp 2	24	41	20				
"	"	"	"	Used 1	23	43	19				
20190506113	06.05.2019	06.05.2019	06.05.2019	Used 2	24	42	20				

Comment:

CHEMIST/SNR.CHEMIST

E. DANGENI
CHIEF CHEMIST